Informal AEC Research and Development Report

GEAP 3717

HIGH POWER DENSITY DEVELOPMENT PROJECT

FOURTH QUARTERLY PROGRESS REPORT
JANUARY - MARCH 1961

Prepared for the

ATOMIC ENERGY COMMISSION

By

L. K. Holland

Contract No. AT(04-3)-361

April 1, 1961

GENERAL ELECTRIC

ATOMIC POWER EQUIPMENT DEPARTMENT

SAN JOSE, CALIFORNIA

DISCLAIMER

Informal AEC
Research and Development Report
HPD Consumers Power
GEAP 3717

HIGH POWER DENSITY DEVELOPMENT PROJECT

FOURTH QUARTERLY PROGRESS REPORT

JANUARY - MARCH 1961

PREPARED FOR THE ATOMIC ENERGY COMMISSION

BY L. K. HOLLAND

UNDER CONTRACT NO. AT(04-3)-361

GENERAL ELECTRIC COMPANY
ATOMIC POWER EQUIPMENT DEPARTMENT
SAN JOSE, CALIFORNIA

April 1, 1961

APPROVED BY: D N Imhoff
D. H. Imhoff, Manager
Engineering Development

S. Levy
S. Levy
Project Engineer

LEGAL NOTICE

EXTERNAL REPORT DISTRIBUTION LIST

	No. of Copies
U. S. Atomic Energy Commission Washington 25, D. C. Attention: Chief, Water Reactors Branch Civilian Reactors, DRD	(5)
U. S. Atomic Energy Commission Washington 25, D. C. Attention: Chief, Water Systems Project Branch Army Reactors, DRD	(1)
U. S. Atomic Energy Commission Washington 25, D. C. Attention: Chief, Fuels and Materials Development Branch Nuclear Technology, DRD	(1)
General Nuclear Engineering Corporation P.O. Box 245 Dunedin, Florida Attention: J. M. West	(1)
Combustion Engineering, Inc. Nuclear Division Prospect Hill Road Windsor, Connecticut Attention: W. H. Zinn	(1)
Westinghouse Electric Corporation Atomic Power Department P.O. Box 355 Pittsburgh 30, Pennsylvania Attention: Dr. W. E. Shoupp	(1)
Allis-Chalmers Manufacturing Company Atomic Energy Division Milwaukee 1, Wisconsin Attention: C. B. Graham	(1)
Allis-Chalmers Manufacturing Company Nuclear Power Department P.O. Box 8697 Washington 11, D. C. Attention: H. Etherington	(1)
Northern States Power Company Minneapolis 2, Minnesota Attention: D. F. McElroy	(1)

EXTERNAL REPORT DISTRIBUTION LIST
(continued)

	No. of Copies
U. S. Atomic Energy Commission Chicago Operations Office 9800 South Cass Avenue Argonne, Illinois Attention: C. A. Pursel, Director Reactor Engineering Division	(5)
U. S. Atomic Energy Commission San Francisco Operations Office 2111 Bancroft Way Berkeley, California Attention: W. H. Brummett, Jr., Director Contracts Division	(2)
Attention: G. F. Helfrich, Director Reactor Division	(1)
Meyer Novick Argonne National Laboratory P.O. Box 2528 Idaho Falls, Idaho	(1)
Hoylande D. Young, Director Technical Information Division 9700 South Cass Avenue Argonne, Illinois	(1)
W. C. Cooper Consumers Power Company 212 W. Michigan Avenue Jackson, Michigan	(5)
U. S. Atomic Energy Commission Technical Information Service Extension P.O. Box 62 Oak Ridge, Tennessee	(3) (plus master)

ACKNOWLEDGEMENT

The Research and Development Program associated with the Consumers Big Rock Plant and sponsored by the AEC is being conducted by the General Electric Company, with the following personnel contributing to the project during the fourth quarter.

Project Engineer	S. Levy
Fuel Development	T. J. Pashos
Fuel	J. W. Lingafelter W. D. Fowler W. R. De Hollander E. A. Lees C. M. Ryer
Instrumented Assembly	A. G. Dunbar A. C. Duckart E. Janssen
Vibration Testing	E. P. Quinn
Nuclear Development	S. Levy
Stability and Transient Performance	L. K. Holland J. M. Case
Heat Transfer and Fluid Flow	E. E. Polomik
Physics Development	D. L. Fischer
Physics Studies	R. K. Haling C. L. Miller M. L. Couchman H. C. Bollinger
300 MW Conceptual Design	C. L. Miller M. L. Couchman V. G. Grayhek
Computer Scheduling of Control	E. S. Beckjord W. H. Harker D. V. Steward
Operational Planning and Test Coordination	L. K. Holland

TABLE OF CONTENTS

ILLUSTRATIONS

TABLES

INTRODUCTION

The AEC-Consumers High Power Density R & D Program has been in progress since February 1960, with the fuel development portion starting at that time, followed in April with the initiation of the remainder of the program. Fuel design and fabrication has proceeded essentially on schedule, while irradiation and examination phases have lagged due to the recent VBWR operating history. It is expected that with the presently anticipated VBWR operation schedule, outlined elsewhere in this report, further irradiation program delays should be insignificant and the overall progress of the development work will proceed unimpaired. This effort can be described by the following outline of the major tasks and their objectives, whose progress is summarized and detailed in this report.

1. Task IA - High Power Density Fuel Development

   This task will evaluate the feasibility and the performance of a partial reactor core operating in the VBWR at high power density and utilizing fuel elements manufactured from available fabricating processes.

2. Task IB - Fuel Fabrication Development

   Design, fabrication, irradiation and examination of high power density fuel elements with potentially low fabrication costs is the objective of this task.

3. Task II - Stability and Heat Transfer Development

   This task will evaluate analytically and by test the transient behavior and stability characteristics of the Consumers Big Rock Reactor, and will determine by test the heat transfer and fluid flow characteristics of the core, using elements simulating core characteristics.

4. Task III - Physics Development

This task involves the physics evaluation of control requirements and hot spot reduction; the physics and engineering conceptual design of a 300 MWe high power density reactor; and the physics and engineering required to design, procure and put into operation a computer for scheduling control.

5. Task IV - Operational Planning and Test Coordination

The coordination of the R & D program between tasks, with Design Engineering, and with the AEC and Consumers is a major function of this task, as is the design of tests and the procurement of instrumentation.

SUMMARY

The fourth quarter of effort applied to the Consumers R & D Program is summarized by Task in the following.

Task IA - High Power Density Fuel Development

1. Twenty-two of the twenty-four high power density VBWR fuel assemblies accumulated approximately 400 MWD/T exposure during the reporting period. Eleven fuel assemblies were inspected after accumulating this exposure, and were observed to be in good condition.
2. Two instrumented fuel assemblies were completely fabricated and the instrumentation calibrated in an out-of-reactor flow facility at cold, hot, and boiling conditions. They are now ready for insertion in VBWR.
3. Recording, indicating, and control instrumentation associated with the instrumented assemblies was completed and laboratory checked. This includes the "backflow" system used in conjunction with the pressure sensors.
4. Preparations to install the instrumented assembly equipment in the VBWR enclosure and control room are about 60% complete and will be finished by about May 1. Signal cables, enclosure penetration, quick disconnect and seal connectors are complete and installed.

Task IB - Fuel Fabrication Development

1. A final rolling run was performed with good success for the purpose of producing a tandem rolled fuel bundle for irradiation testing. No further work on the tandem rolling process is presently planned.
2. Swaging parameters have been established for multi-pass cold swaging of 10 mil, 12 mil, and 15 mil thick stainless steel clad fuel rods. Fuel assembly 2s was fabricated using these cold swaging techniques. Fuel rod densities of 92% ±1% were achieved.

3. Fuel assembly 1S was completed, fabricated by swaged pellet techniques established for 12 mil thick stainless steel cladding and simulated unground pellets.

4. Inspection of purposely defected powder compacted fuel specimens after 570 hours of erosion flow testing was completed. Results of visual examination indicated that only small amounts of UO_2 had been eroded.

5. The work on vibratory compacted fuel rods was devoted to the study of binary and ternary fused UO_2 powder mixes. Relationships were established between the density of filled rods and composition of various binary and ternary mixes, using fused 3.5% enriched UO_2. As a result of using this material, a large sensitivity of the system to UO_2 particle size and shape and rod size has been shown to exist.

6. Manufacture of drawn cup type fuel rod end plugs has demonstrated that a unit cost of approximately 4¢ each is possible. Mechanical and corrosion testing of cup type end plugs has been completely satisfactory.

7. Design is complete on ten of the twelve special HPD-VBWR fuel assemblies. Two of these assemblies have been fabricated and delivered for VBWR irradiation testing.

8. A series of vibration tests on a 36 rod Consumers type element have indicated less than .001" vibration amplitude of the instrumented rod in rated operating flow conditions of steam and water. By varying the spacer configuration, displacements up to .007" were observed.

Task II - Stability, Heat Transfer and Fluid Flow

1. The 50 MW Big Rock Reactor, for operation at rated conditions, has been analyzed and found to be stable. Both the hydrodynamic analysis and the reactor-recirculation loop analysis indicate substantial stability margins based on normal feedback analysis criteria.

2. Flow stability and pressure-drop tests were completed on the air-water flow facility simulating the core, reactor head, risers and steam drum. Baffles placed above the core have been investigated to select the best means of minimizing non-uniform distribution and slug-flow effects.
3. The out-of-reactor heat transfer test section is now under construction and is scheduled to go into operation in June.

Task III - Physics Development

1. Further one-dimensional studies have been made to investigate local power flattening through reductions in enrichment near water gaps. The time dependent effect of burnup is to increase slightly with time the relative power in the fuel rods adjacent to the gap. A more important burnup effect can result from the local perturbations of inserted control rods, increasing the local peaking factor by 10% for the case studied.
2. Studies of gross radial power distribution indicate that proper radial distribution of partially burned fuel can produce desirable radial power shapes. Ultimately, calculations of time dependent power distribution must reflect the actual three-dimensional nature of the operating reactor.
3. The physics analysis of the reactor core for a large 300 MWe high power density conceptual design has been completed and a report issued (GEAP 3649).
4. A topical report is now being prepared for issuance describing the present status of the efforts involving the scheduling computer. Incentives for the computer have been investigated and the basic functions to be performed have been defined and equations written. These studies will next be refined and utilized in the formulation of specifications for the procurement of the scheduling computer. Two important results of the availability of such a computer during reactor operation will be to maximize fuel burnup and to permit safe operation closer to burnout and other limits.

Task IV - Operational Planning and Coordination

1. Procurement of instrumentation and test facilities associated with the instrumented assemblies for VBWR is 95% complete through this quarter.
2. Requirements imposed on Design Engineering to assure R & D program fulfillment were reviewed regularly. Safety valve requirements were established for the range of operating pressures anticipated.
3. The Third Quarterly Progress Report, GEAP 3632, two monthly reports, and the required task descriptions and cost estimates for AEC Form 189 were prepared and issued.
4. A topical report, "The Design and Fabrication of High Power Density Fuel Assemblies for VBWR Irradiation Testing," GEAP 3609, by J. W. Lingafelter and W. D. Fowler, was issued during this quarter. Two additional reports were prepared for issuance subject to AEC approval.

TASK IA - HIGH POWER DENSITY FUEL DEVELOPMENT

1. TASK OBJECTIVE

A partial core consisting of 24 high power density fuel elements designed and fabricated by existing manufacturing processes will be irradiated in VBWR to study its performance and explore its feasibility. The effect of variations in structure, geometry, fabricating processes and mechanical features will be evaluated in terms of operation of 90 kw/l average power density to 10,000 MWD/T average exposure. Instrumented assemblies capable of measuring flow, temperature, pressure drop, and flux level will be utilized.

2. FUEL IRRADIATION

The twenty-two high power density VBWR fuel assemblies have accumulated a total exposure of approximately 400 MWD/T to date. Fuel exposure has been limited to this low value due to reactor outages in excess of what originally had been anticipated. The VBWR has been down during March, and presently is scheduled to resume operation in April.

3. INSPECTION OF TASK IA FUEL ASSEMBLIES

During the period February 20 to March 10, 1961, the following Task IA assemblies were inspected and the following observations were made. All inspections were performed in the VBWR fuel storage building using the 1X and 5X periscope.

Assemblies 2-101 and 2-102 (1A and 2A) - These assemblies were inspected and no damage or defects were noted. Welds on the tie plates and fuel rods were in good condition, the spacer was in place and the exterior of the rods appeared to have a uniform coating of oxidation. Bundle 2-102 had what

appeared to be a 1/16" diameter dent on rod #557 immediately below the spacer location.

Assembly 2-108 (4C) - Spacer was cocked slightly from a horizontal plane but the assembly is in good condition. No corrective action was necessary.

Assembly 2-111 (3D) - Excellent condition.

Assemblies 2-113 (1E), 2-114 (2E), 2-115 (3E), and 2-117 (5E) - were visually inspected for broken tie wires and none were broken. In observing these assemblies (without use of the periscope), they all appeared to be in good condition.

Assembly 2-116 (4E prototype) - One spacer tie wire was broken; otherwise the assembly was in good condition. The tie wire has been replaced remotely.

Assembly 2-119 (1F prototype) - One spacer tie wire was broken for the second time, otherwise the assembly was in good condition. This tie wire has been replaced and the assembly is acceptable for further irradiation. On March 18, 1961, subsequent to the tie wire replacement, the assembly was inadvertently dropped from a height of approximately 10 feet, in water, during handling operations in the VBWR spent fuel pit. A visual inspection of the assembly was performed and it did not appear to have suffered any deformation or scratching of fuel rods as a result of its fall. The assembly was then trial fitted in a channel to determine if the tie plates had been distorted. The assembly went into the channel in a normal fashion. This assembly will be placed in the core for further irradiation.

Assembly 2-123 (3G) - This assembly was inspected because a report that a lead brick had been accidentally dropped in the spent fuel pit, and it came

to rest in the fuel storage rack adjacent to 2-123 and a control rod. Lead scrappings were present on the spiral pin that holds the extension handle to the top tie plate. No effects were noted on the fuel rods, tie plates, or spacer. The fuel assembly was trial fitted in a channel without trouble. It can only be surmised that assembly 2-123 did not receive the full impact of the brick. The assembly will receive further irradiation at the next VBWR startup.

Assembly 2-124 (4G) - Excellent condition.

4. INSTRUMENTED ASSEMBLIES

Instrumented assemblies 2-118 (6E) and 2-120 (2F) are 95% complete. The remaining work to be completed on the two assemblies is the addition of the signal cable flexible lead-wire transitions. These transitions convert the existing mineral insulated stainless steel sheathed signal cables into flexible insulated signal cables.

Instrumented Assembly 2-118 (6E) - This assembly contains the short (3') fuel rods and incorporates inlet and outlet flowmeters. Figures 1 through 6 are photographs at various stages of assembly and show the several sensors incorporated.

The overall instrumented assembly fuel, components, and sensors are illustrated in Figure 1. The lower flowmeter housing and nosepiece are shown at the right. Above this piece fits the fuel assembly, shown with four corner rods, the center instrument lead tube, the tie-plates, and the wire spacers. On the table just below are the in-core ion chambers to be placed at quarter points along the fuel bundle. The parts at the right include the lower thermocouple assembly and the lower pressure tap. To the left end of the assembly is

shown the upper flowmeter housing with a pressure tap protruding toward the fuel and the upper three-thermocouple assembly in place. The completed assembly is housed in the channel shown at the bottom of the picture.

Figures 2, 3, and 4 show greater detail of the lower portion of this assembly. Figure 2 illustrates the unassembled channel, nosepiece, thermocouple assembly, flowmeter, fuel bundle, thermocouple and pressure sensor assembly, and the flowmeter pickup coil. Figures 3 and 4 picture the assembled components close-up. Figures 5 and 6 show the partially assembled upper flowmeter, fuel bundle, pressure taps, and thermocouples. The fuel hanger brackets are also visible.

Instrumented Assembly 2-120 (2F) - This assembly contains long (about 5') fuel elements, the upper portion not containing active fuel, to more nearly simulate the configuration of Big Rock Reactor fuel. Except for the upper flowmeter and pickup coil, this assembly contains the same instrumentation as 2-118. Figures 2, 3, and 4, therefore, are representative of this assembly also.

The overall, partially assembled bundle is shown in Figure 7, indicating the long fuel assembly and the upper fuel hanger. The one-half inch hollow center rod houses three neutron flux sensors at quarter points along the active fuel region. Figure 8 illustrates the outlet thermocouples, transition housing, and sensor signal leads.

General Instrument Assembly Details - Outwardly the two instrumented fuel assemblies appear identical and, for installation purposes, have exactly the same physical outside dimensions. A completed instrumented assembly is shown in Figure 9. Specific details of the upper fuel assembly, such as the hold down clamp, rigging support bar, disassembly bolts and signal cable

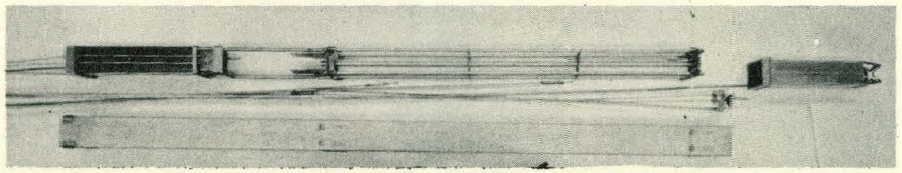

FIGURE 1 - PARTIALLY ASSEMBLED INSTRUMENTED ASSEMBLY 2–118 (6E)

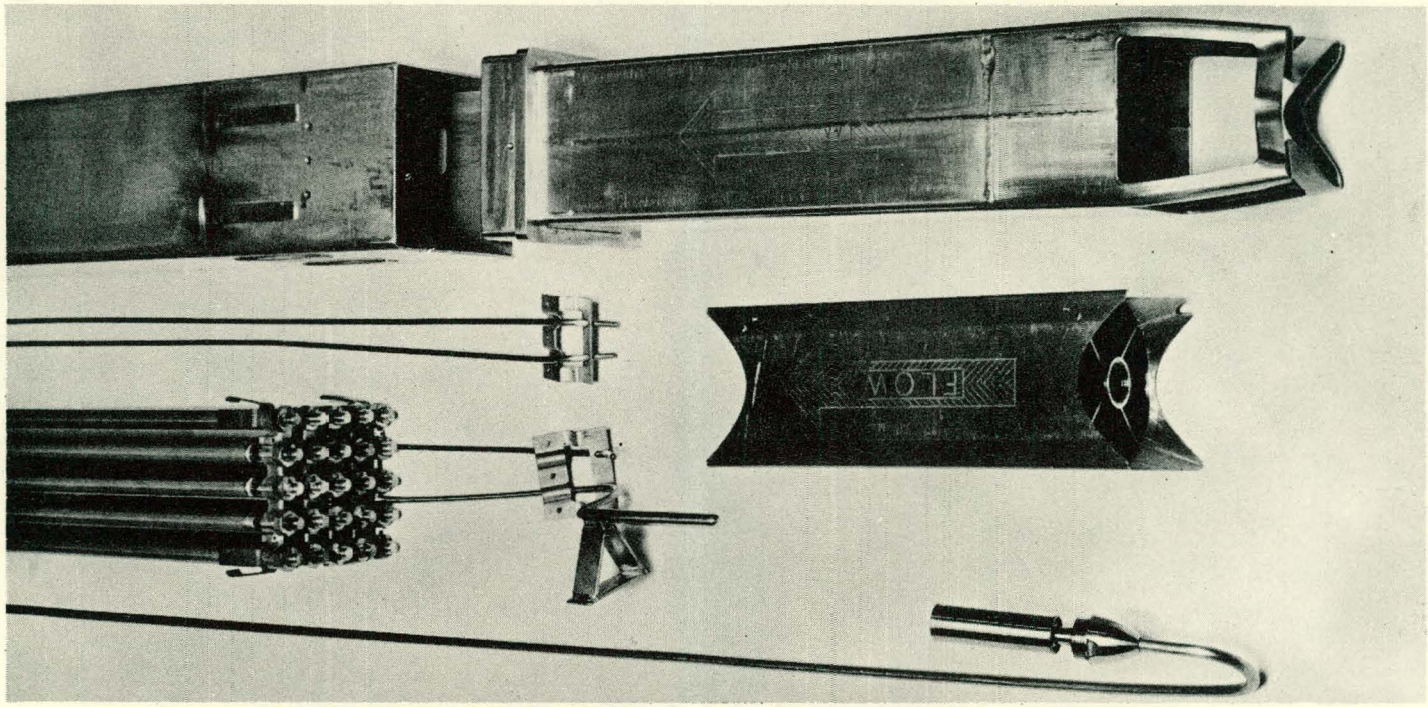

FIGURE 2 - LOWER PORTION OF PARTIALLY ASSEMBLED ELEMENT 2–118

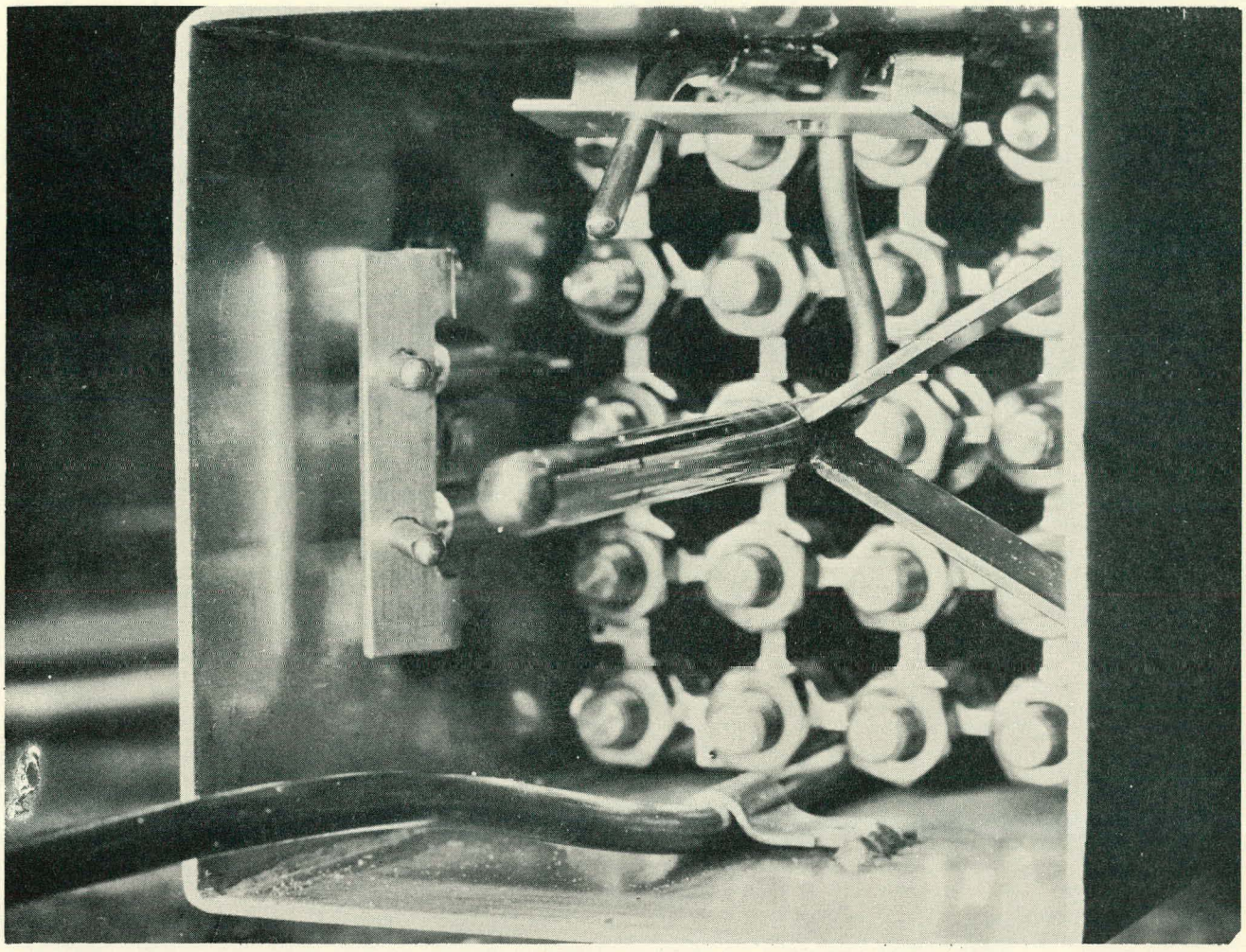

FIGURE 3 - CLOSEUP LOWER END VIEW OF ASSEMBLY 2–118

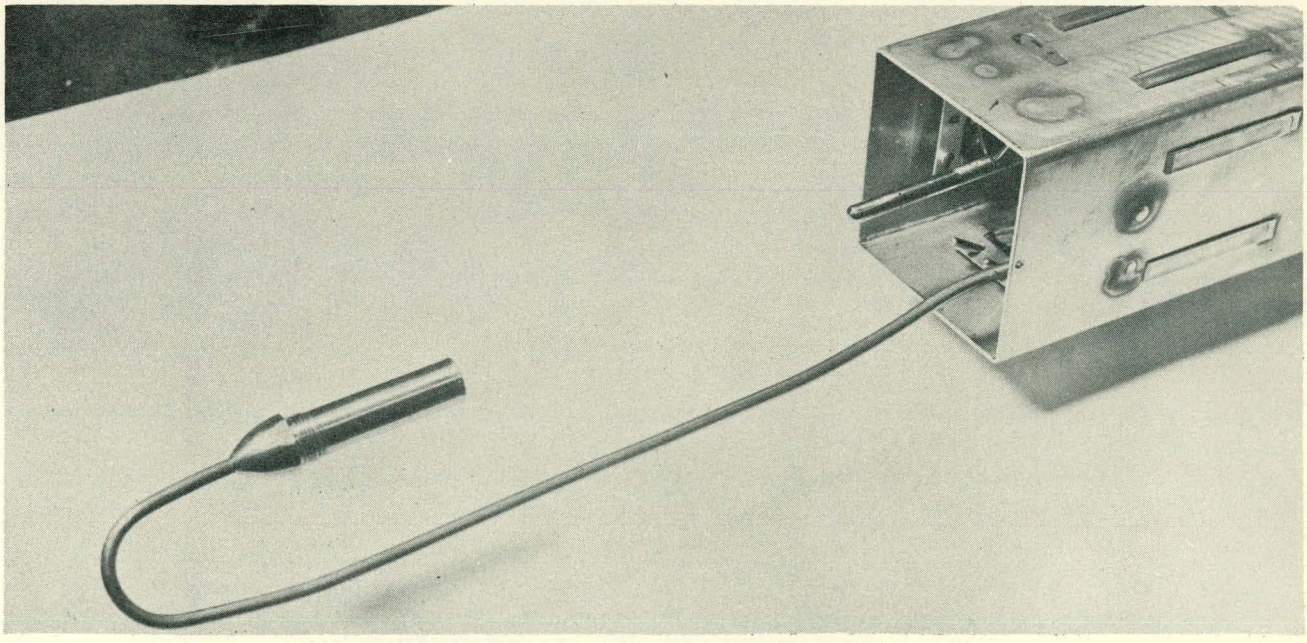

FIGURE 4 - FLOW SENSOR PICKUP COIL AND LOWER END OF ASSEMBLY 2–118

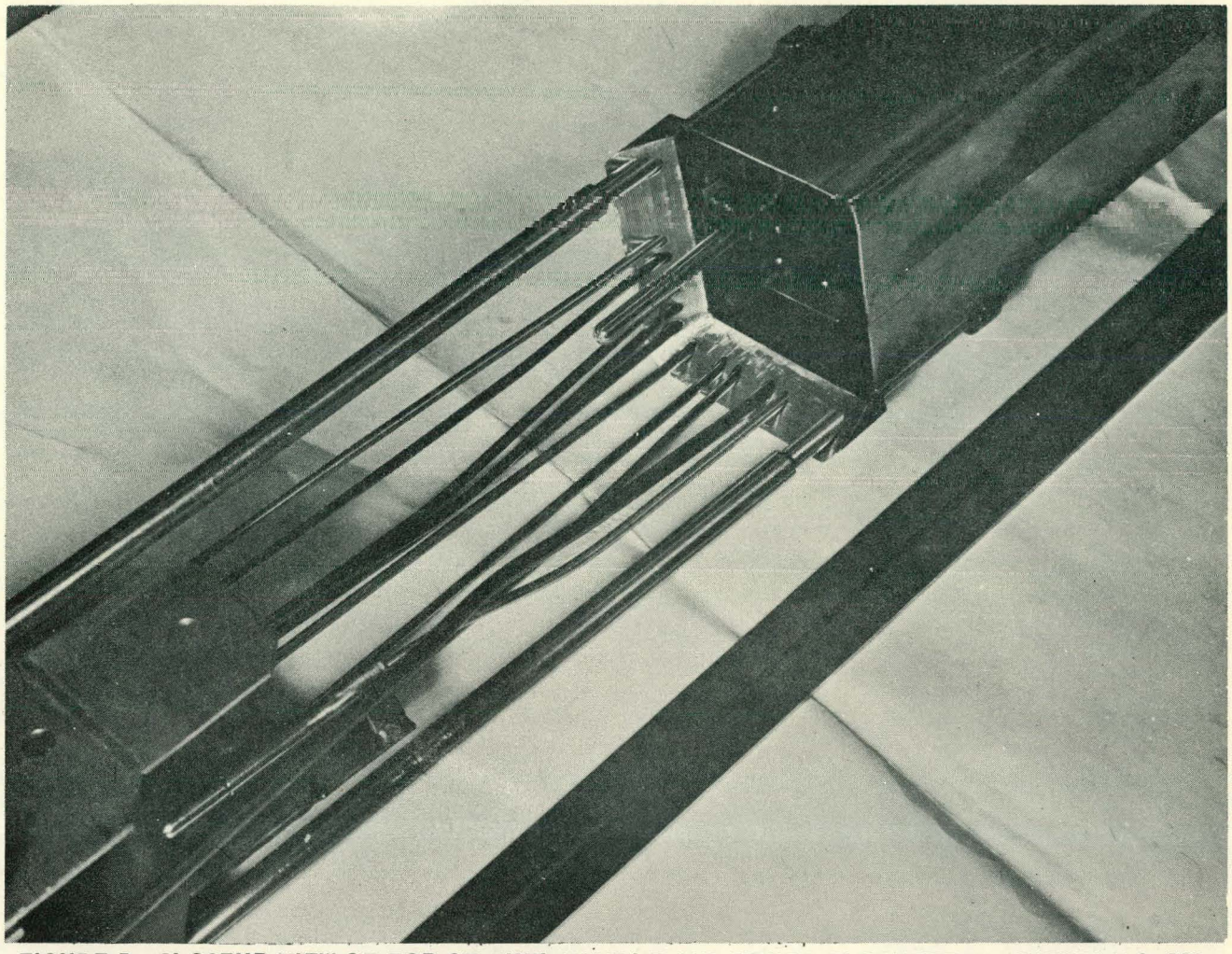

FIGURE 5 - CLOSEUP VIEW OF TOP OF FUEL BUNDLE AND UPPER FLOWMETER - ASSEMBLY 2–118

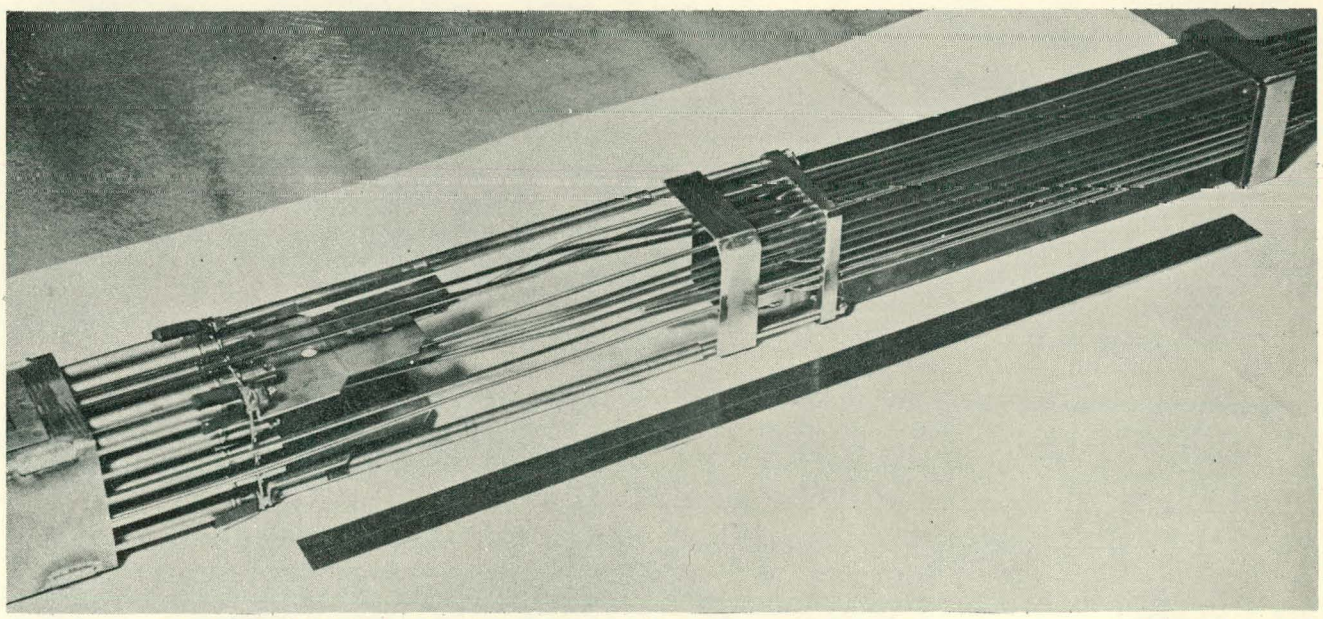

FIGURE 6 - PARTIAL ASSEMBLY VIEW OF FUEL BUNDLE AND UPPER FLOWMETER - ASSEMBLY 2–118

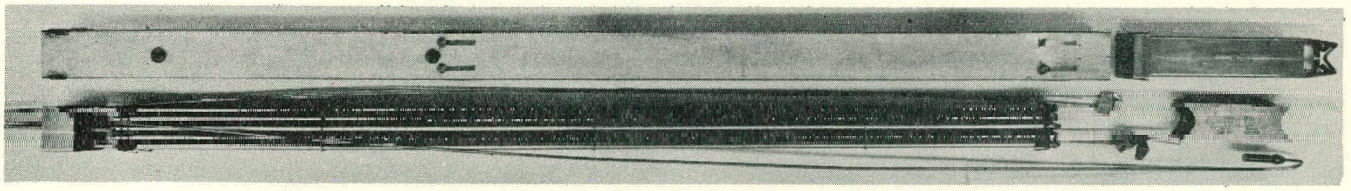

FIGURE 7 - PARTIALLY ASSEMBLED INSTRUMENTED ASSEMBLY 2–120 (2F)

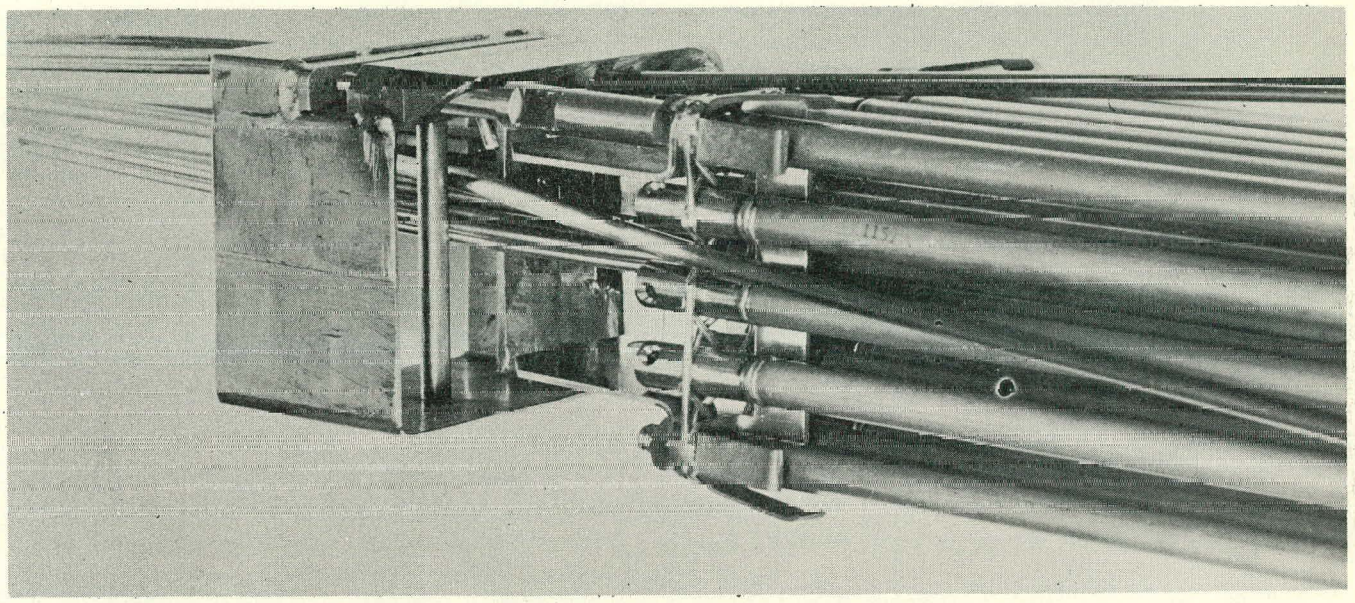

FIGURE 8 - TOP OF PARTLY ASSEMBLED BUNDLE 2–120

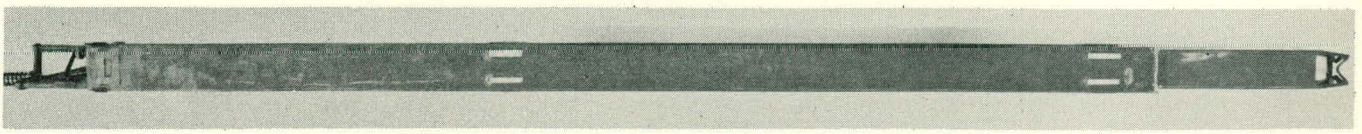

FIGURE 9 - COMPLETED INSTRUMENTED ASSEMBLY

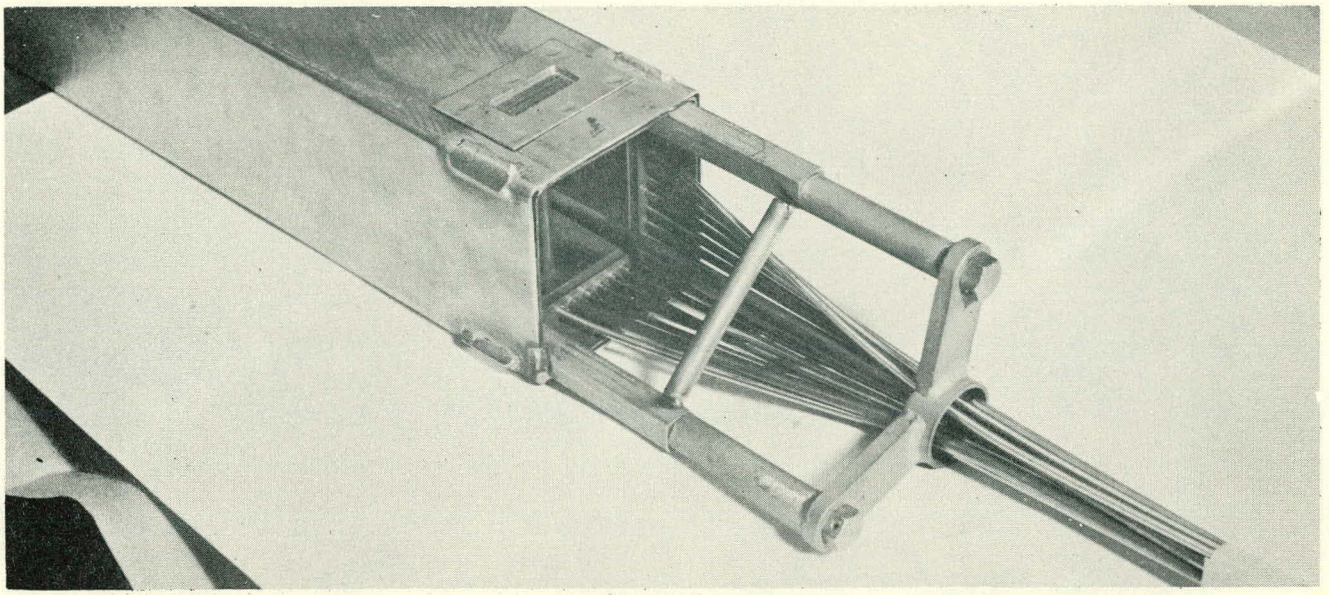

FIGURE 10 - INSTRUMENT LEAD BUNDLE EXIT FROM TOP OF INSTRUMENTED ASSEMBLY

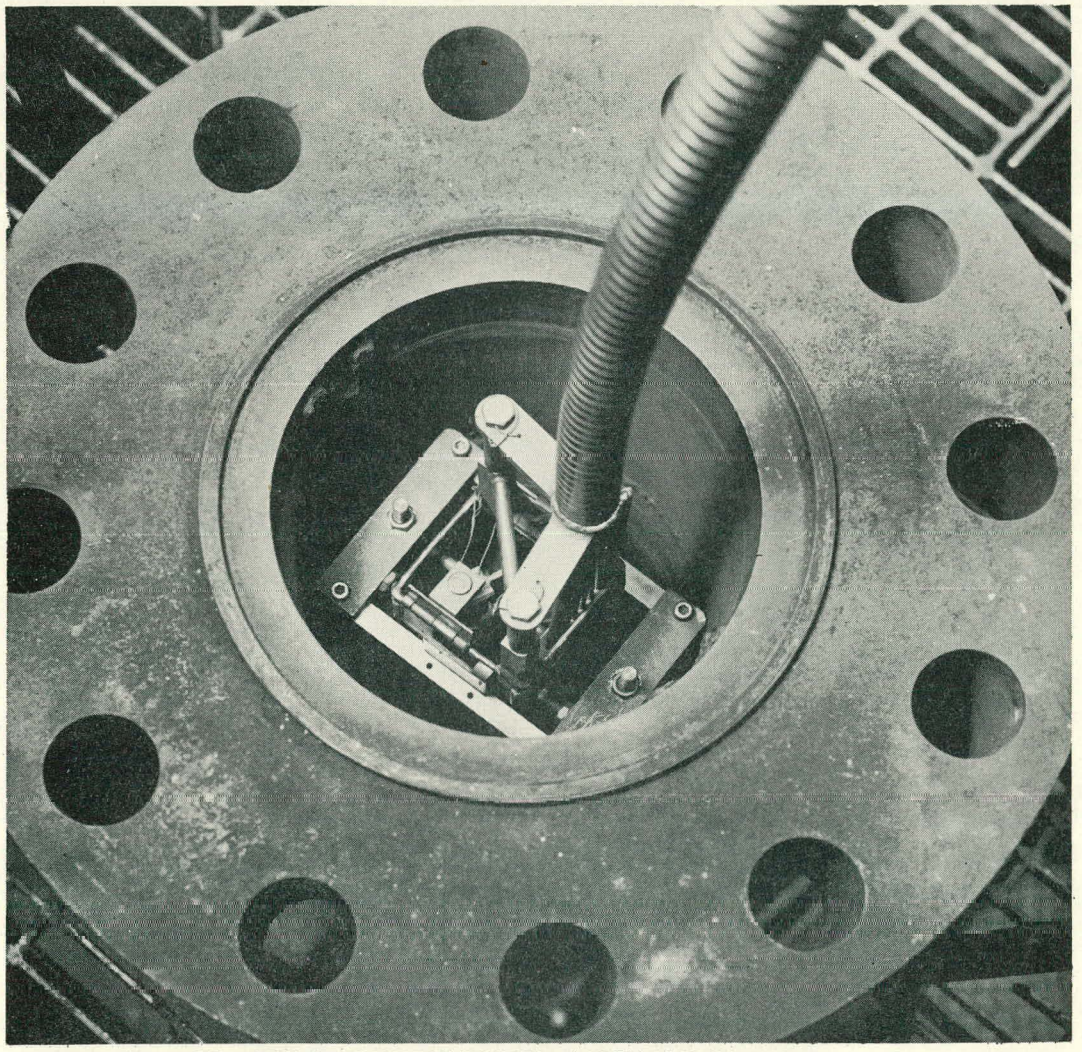

FIGURE 11 - TOP VIEW OF INSTRUMENTED ASSEMBLY IN CALIBRATION FACILITY

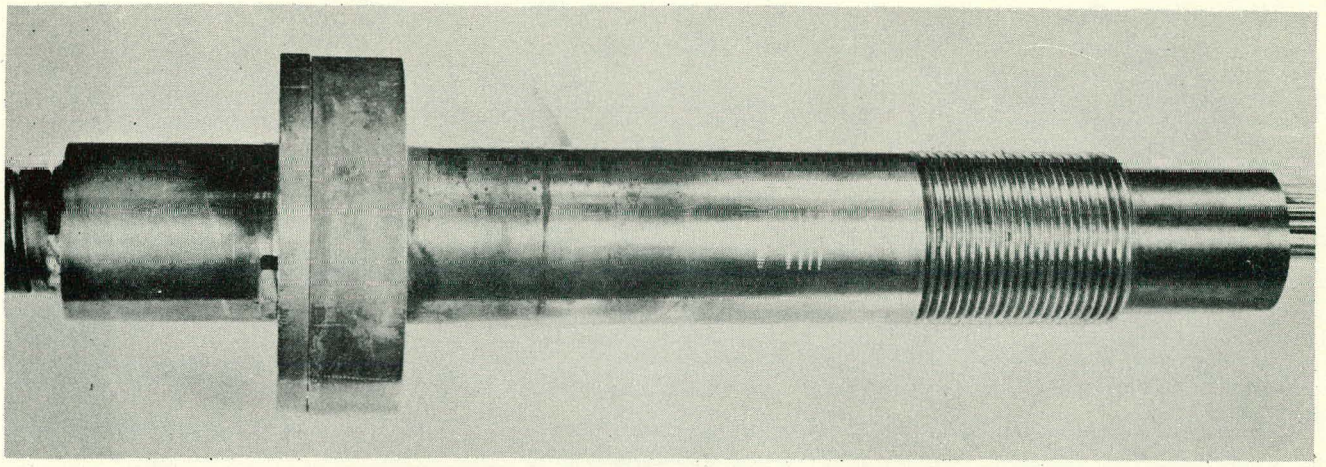

FIGURE 12 - REACTOR VESSEL PENETRATION SEAL PLUG

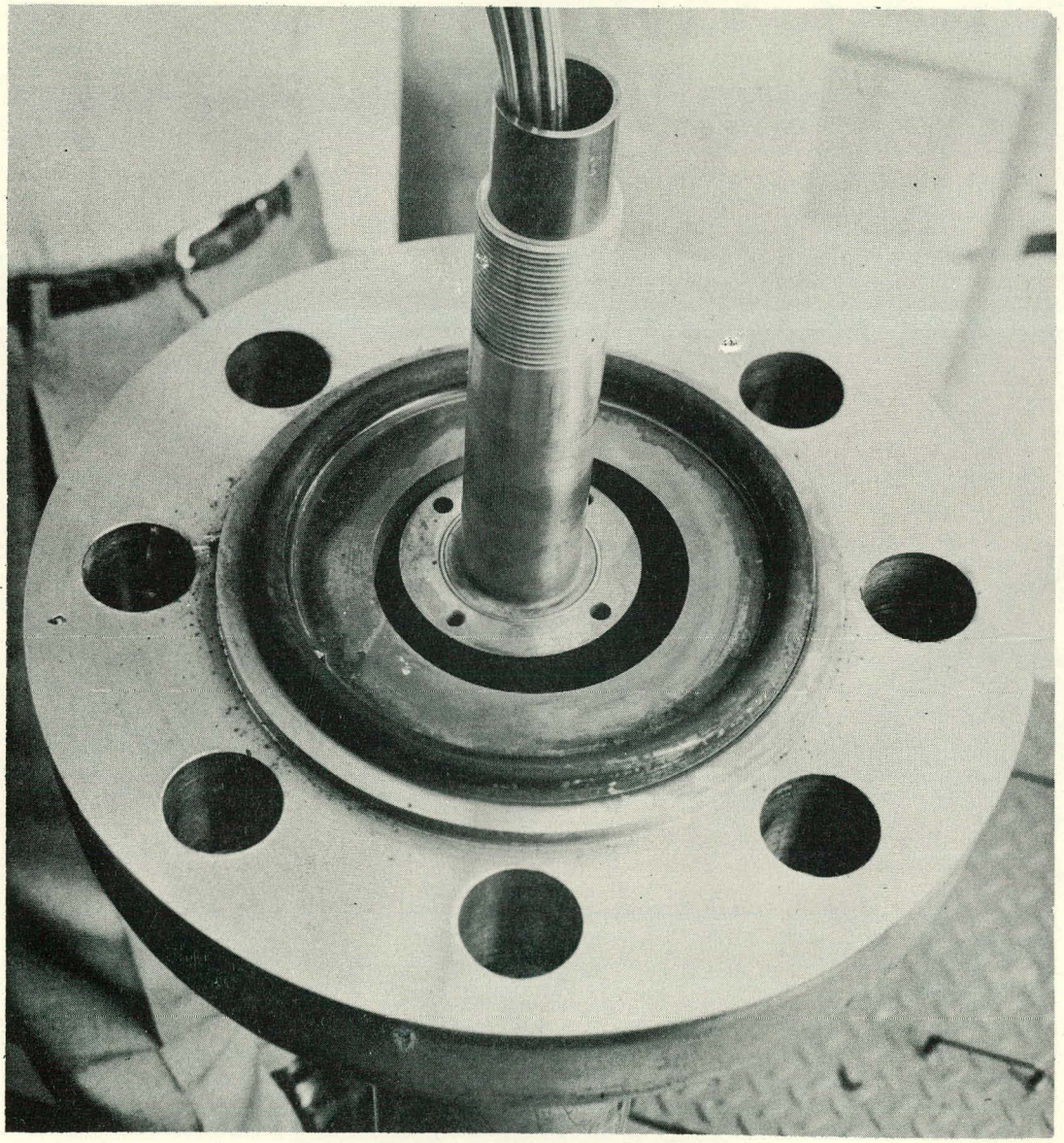

FIGURE 13 - REACTOR VESSEL PENETRATION PLUG SHOWING PRESSURE SEAL

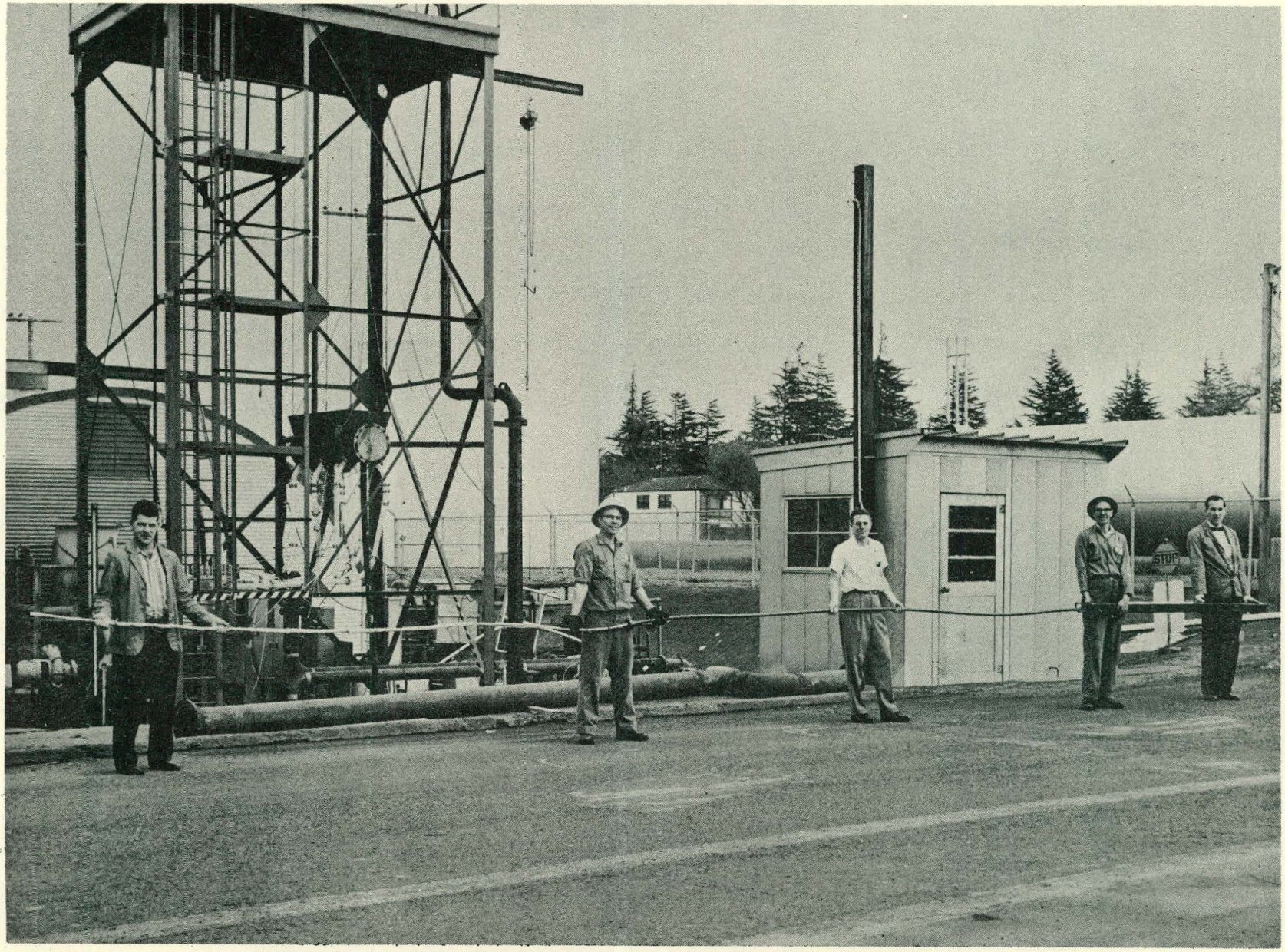

FIGURE 14 - COMPLETED INSTRUMENTED ASSEMBLY AND INSTRUMENT CABLE

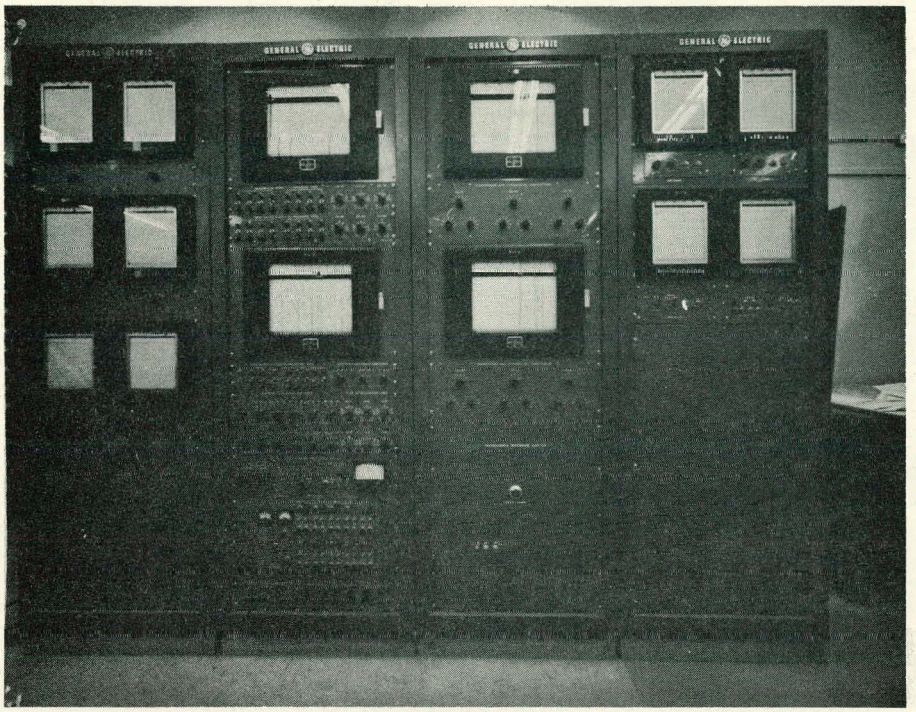

FIGURE 15 - CONTROL ROOM INSTRUMENT PANELS FOR INSTRUMENTED ASSEMBLIES

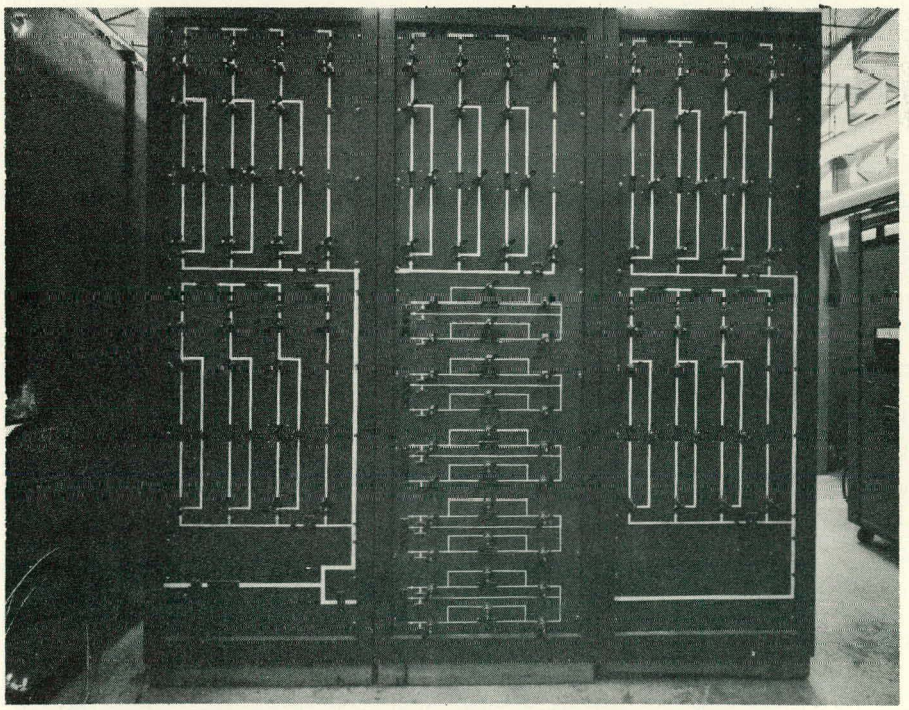

FIGURE 16 - REACTOR ENCLOSURE INSTRUMENT PANELS FOR INSTRUMENTED ASSEMBLIES

protection Rex-Flex sheath are illustrated in Figures 10 and 11, the latter showing the assembly located in the calibration test facility.

Reactor vessel penetration is accomplished with the seal plug shown in Figures 12 and 13. The small steal "O" ring shown in Figure 13 acts as the pressure seal for each specific assembly, the plug being illustrated inside a larger calibration assembly flange.

A completed assembly is shown in Figure 14. This picture illustrates the instrumented assembly, signal cable protection sheath, flange penetration plug and the measuring sensor signal leads.

Instrumentation Monitoring System - The readout and recording instrumentation cubicles for the control room and reactor enclosure are 100% complete. Control room and reactor enclosure modifications to permit installation of the panels is 60% complete. Reactor enclosure signal cable penetration connectors and cables are installed and pulled through to the control room panel location and to the enclosure panel location.

A. Control Room Instrument Panels

Four instrument cubicles, as shown in Figure 15, house the measuring and monitoring equipment for the instrumented assemblies. Panel No. 1 on the right is the flow monitoring panel. Panel No. 2 is the temperature monitoring panel. Panel No. 3 is the differential pressure and neutron flux monitoring panel. Panel No. 4 is the transient data recording panel.

B. Reactor Enclosure Instrument Panels

Three instrument cubicles, as shown in Figure 16, house the pressure sensing detectors, pressure tap back flow controls and the instrumented assembly enclosure electrical signal junctions.

The graphic panel layout of the back-flow system and the differential pressure measuring system is sectionalized for each instrumented assembly. The differential pressure measuring transducers are located in the lower half of the center panel. Each of the other panels contain individual instrumented assembly back-flow measuring and flow control valves and piping. The panel on the right side serves a dual purpose and provides the electrical junction terminals for the connection of the instrument assembly signal leads to the control room interconnection cables.

Instrumented Assembly Calibration - Each of the instrumented assemblies were installed in the heat transfer and fluid flow test loop for cold, hot (single phase) and hot (two-phase) flow measuring system calibrations. Differential pressure drop data were recorded from both manometers and the instrumented assembly differential pressure measuring equipment.

A. Cold Water Calibration

A cold water flow calibration was performed to check the flow loop reference 2.175" orifice. The orifice calibration at reference temperature of 75°F was performed with the instrumented assembly 2-118 in series with the orifice. Orifice coefficients and instrumented assembly flowmeter data were reduced and plotted (Figure 17, curve for 75°F) for reference use. This data plot indicates the mass flow in pounds per hour versus the flowmeter indication in gallons per minute at 75°F.

B. Hot Water Calibration

Hot water single-phase flow calibration runs were performed utilizing the 2.175" reference orifice. The orifice coefficients were Reynolds number corrected for 545°F hot water. Hot water flowing at 545°F

and pressures in excess of 1000 psia with mass rates in pounds per hour, were recorded and plotted (Figure 17, Curve 545°F) versus instrumented assembly flow rates in gallons per minute.

C. Two-Phase Flow Calibration

Hot water two-phase flow calibration runs were performed to establish the measured instrumented assembly flow at various two-phase flow conditions. Established loop conditions of power input, flow rate in pounds per hour referenced to the loop orifice, temperature, and pressure permitted a specific quality to be maintained for each two-phase run. These two-phase flow data in pounds per hour versus flowmeter indications were recorded and plotted, Figure 18. A direct readout of pounds per hour of steam, quality of the mass flow, and average power generated in the instrumented fuel assembly may be obtained by utilizing the plotted data and the inlet and outlet flow meter indications.

Instrumented fuel assembly sensors and readout equipment characteristics are described and tabulated below. Each of the measuring and monitoring systems have been calibrated against laboratory standards and, as indicated above, the flow measuring and the pressure drop system were calibrated experimentally in a test loop. Individual sensors and systems are a) flow measuring system, b) differential pressure measuring system, c) temperature measuring system, d) neutron flux measuring system and e) transient or continuous data monitoring system. Table I reflects manufacturers' sensor and equipment data, laboratory calibration checks, laboratory response tests, test loop calibration checks, and conservative theoretical calculations.

FIGURE 17

MASS RATE VS. POTTER METER INDICATION

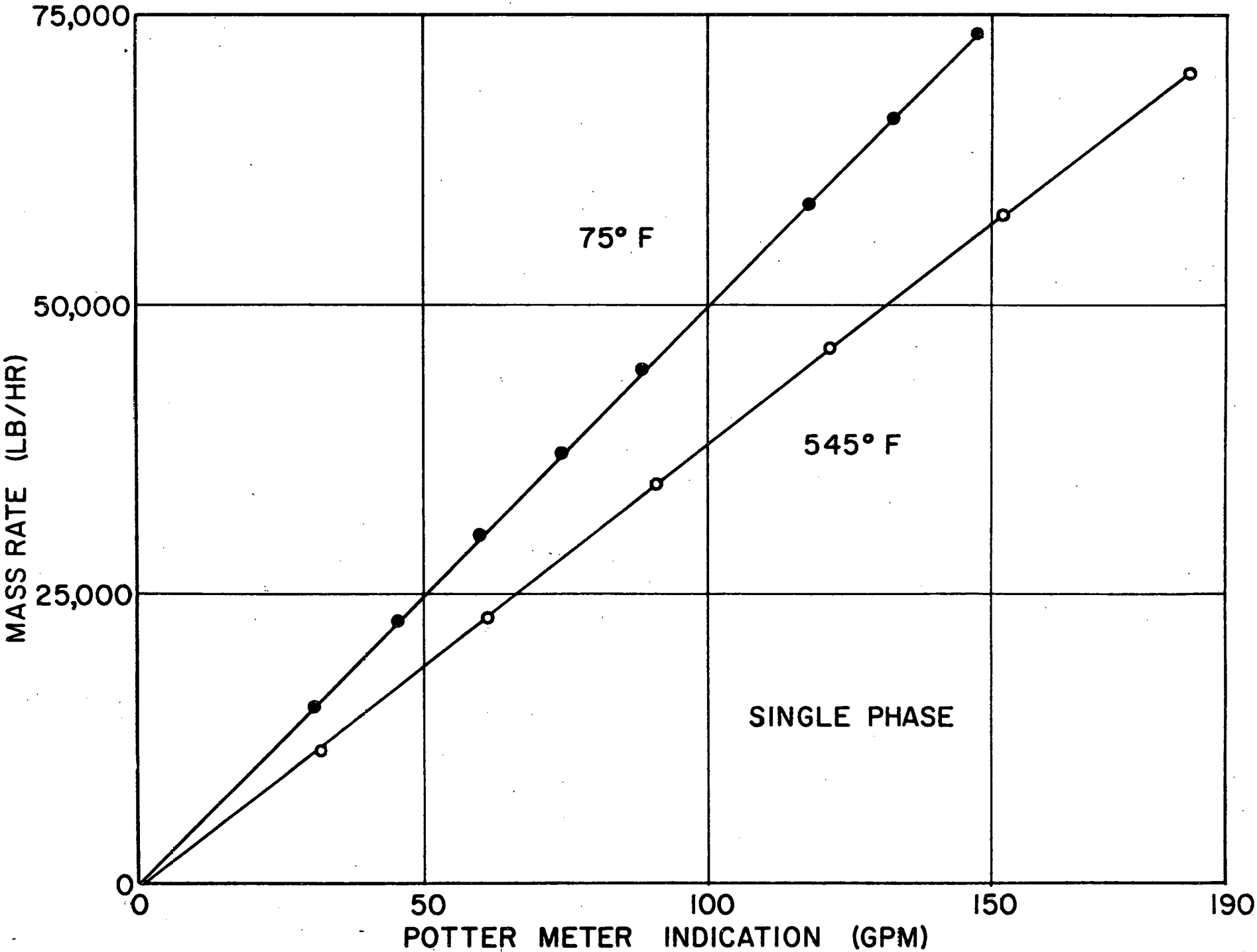

FIGURE 18

STEAM MASS RATE VS. POTTER METER INDICATION

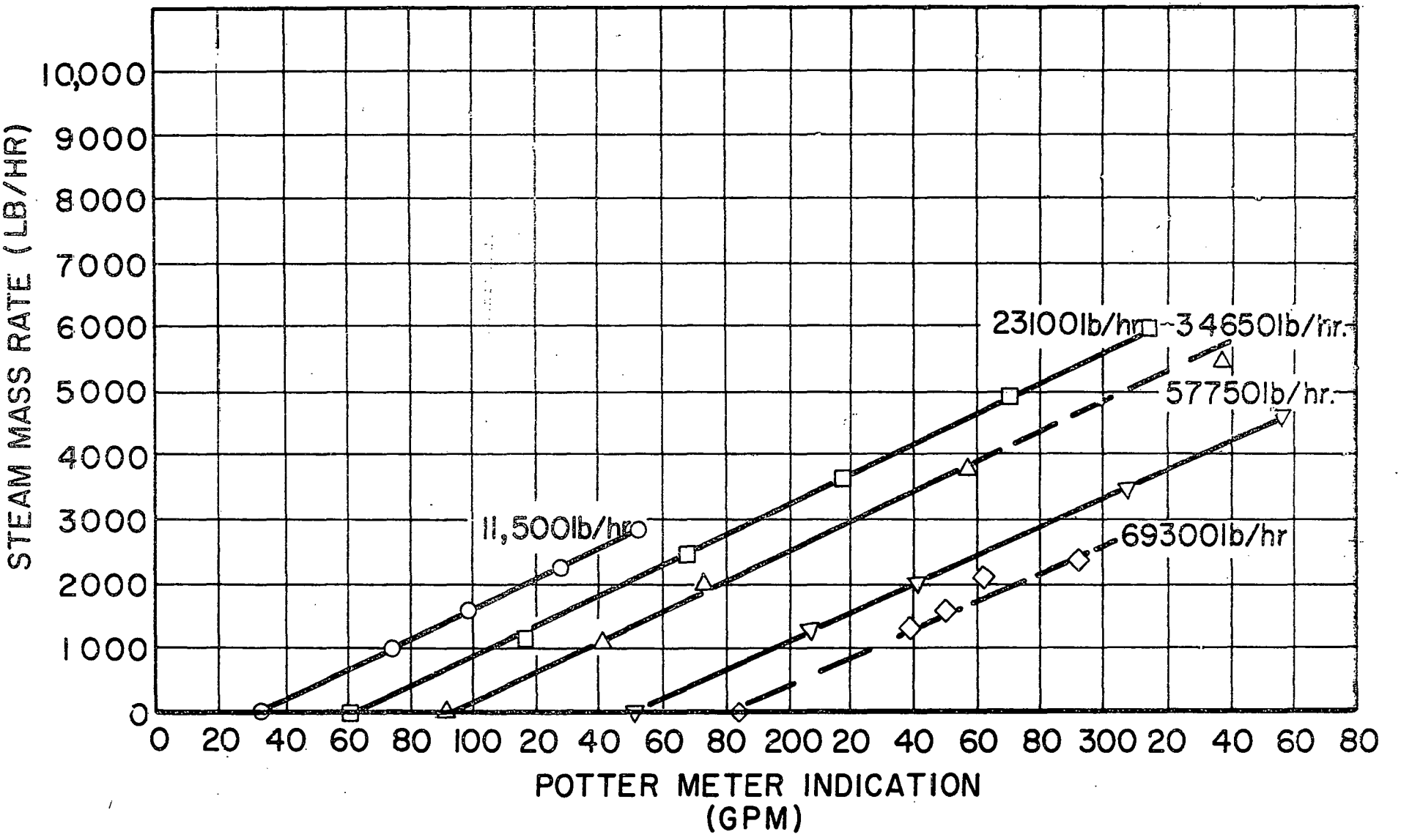

Table I - Sensor and Readout Characteristics

	System	SENSOR Type	SENSOR Response	READ-OUT SYSTEM Type	READ-OUT SYSTEM Range	READ-OUT SYSTEM Resolution	READ-OUT SYSTEM Response	Overall System Accuracy
a)	Flow Measuring System	Potter Turbine	$\leq$ .2 Sec.	Potter Integrator	A)0-200 gmp	± 1%	1.0 Sec.	$\approx$ ± 1.5%
				L & N Recorder	B)0-400 gmp	± 1%		
b)	Differential Pressure System	Pace Reluctance	$\leq$ .1 Sec.	Pace 3000 Cycles per Sec.	A)0-5 psid	± 0.5%		$\approx$ ± 2.0%
				Bristol M.P. Recorder	B)0-1 psid	± 0.5%		
c)	Temperature System	Thermoelectric C/A T.C.	$\leq$ 2 Sec.	Pace REF Junction	A)500-800°F	± 0.3%		$\approx$ ± 2.5%
				Bristol M.P. Recorder	B)0-300°F	± 0.3%		
d)	Neutron Flux System	APED AL-U_{235} Ion Chambers	$\leq$ .1 Sec.	APED Resistance Network	A)2×10^{11} to 2×10^{12}	NV ± 0.5%		$\approx$ ±10-20% *
					B)2×10^{12} to 2×10^{13}			
				Bristol M.P. Recorder	C)2×10^{13} to 2×10^{14}			$\approx$ ± 5% **
e)	Transient System	L & N Recorders	$\leq$ .75 Sec.	L & N Recorders	0 - 7 MV 0 - 100	± 0.5%		$\approx$ ± 0.5% ***

* Best theoretical accuracy as calculated compared to wire irradiation to determine absolute neutron flux.

** Relative accuracy of system based on wire calibration data to establish reference factors for each ion chamber.

*** Accuracy to be maintained, by transient recorder system, of sensor variable signal being monitored.

TASK IB - FUEL FABRICATION DEVELOPMENT

1. TASK OBJECTIVE

The purpose of Task IB is to study the performance in VBWR and in the Consumers Big Rock reactor of fuel assemblies which hold promise of having reduced fuel fabrication costs, long fuel life, and high power density. Approximately twelve fuel assemblies utilizing potential low cost fabrication processes will be designed, fabricated, and irradiated in the VBWR.

The work under Task IB will include investigations of potential reduced-cost fuel element fabrication processes and design, fabrication, irradiation, examination, and performance evaluation of the assemblies. Also included is the mechanical vibration testing of a dummy fuel test section simulating the initial Consumers reference fuel.

2. CALROD TANDEM ROLLING

The rolling process used industrially to produce Calrod-type tubular resistance heating elements is being investigated to determine its applicability for fabricating rod-type fuel elements. In the tandem rolling process, a stainless steel tube filled with fused uranium dioxide is passed through a series of tandem rolls to effect a dense packing of the UO_2 particles. Inherent advantages of the rolling process are high volume of product, size, flexibility, and adaptability to automation.

The objective of the investigation is to determine the effects of processing variables on maximum attainable fuel rod density with the tandem rolling process, and subsequently fabricate fuel rods for irradiation testing.

The tandem rolling of fuel rods has been performed using a production rolling mill having ten sets of roll pairs to effect a 35% reduction in cross-sectional area of the fuel rod (Figure 19).

Based on the results from five early runs with natural UO_2 fuel rods (reported in 3rd Quarterly Report, GEAP 3632), a final rolling run was performed March 25 and April 1. The purpose of this run was to produce fuel rods with enriched UO_2 for irradiation testing (for special fuel assembly 3-S). Pertinent facts about the rolled enriched fuel rods are tabulated in Table II.

Table II

TANDEM ROLLING DATA FOR ENRICHED FUEL RODS

Starting rod diameter	0.502"
Starting rod length	30.50"
Starting tube wall thickness	0.015"
UO_2 powder	Spencer Fused Grade(1)
UO_2 powder enrichment	3.5%
Rolling rate	45 ft/min
Finished rod diameter	0.402"
Finished rod length, avg.	38.25"
Number rods rolled	26
Density of rolled rods, % T.D., max.	89.6
Density of rolled rods, % T.D., min.	87.8
Density of rolled rods, % T.D., avg.	88.7

(1) Screen analysis:

Mesh Size	w/o	Mesh size	w/o
6/8	8	28/35	11
8/10	8	35/48	7
10/14	16	48/65	4
14/20	25	65/100	3
20/28	16	-100	2

The fuel rods were prepared and rolled in the following manner:

(1) Cut tubing to length (30.50").

(2) Wash, rinse, and dry.

(3) Weld collapsible-type end plug to one end.

(4) Load 650 grams 3.5% UO_2 to 30" (687% T.D.)

(5) Evacuate rods, backfill with helium

(6) Weld collapsible-type end plug to second end

(7) Full length rod X-ray

(8) Helium leak-check welds

(9) Roll to 0.400 diameter

(10) Straighten

(11) Full length rod X-ray

(12) Helium leak check

The rods will be assembled into special fuel assembly 3-S, which is scheduled for completion by April 15, 1961. Quality fuel rods were produced by the tandem rolling process for irradiation testing. The process, at present, does not appear capable of producing rolled rod UO_2 densities over 90% T.D. Further work on tandem rolling will be limited, but includes hot rolling MgO-filled samples and cold rolling rods filled with UO_2 loaded to 85% initial density.

3. SWAGED POWDER FUEL

The rotary swaging process is being investigated for fabricating dense UO_2 filled rod-type fuel elements. The swaging process presently under investigation employs a two-die design. Future plans are to investigate the use of a four-die design. In the swaging process, stainless steel tube filled with fused UO_2 is passed through revolving split die (2 parts)

that oscillates back and forth radially while it rotates. This action produces a rapid series of hammer blows that effect a dense packing of the UO_2 particles inside the tube.

Process development work is underway to determine swaging parameters necessary to fabricate swaged fuel rods clad with 8, 10, 12, and 15-mil thick stainless steel.

Swaging parameters have been established for multi-pass cold swaging of 10, 12, and 15-mil thick stainless steel clad fuel rods. Feed rate, die design, starting UO_2 particle size distribution have been established to consistantly produce fuel rods with UO_2 density from 92% to 94%.

Fuel bundle 2-S (Figure 20) was fabricated by this swaging technique over fused UO_2. Thirteen of the rods are clad with 0.015" type 304 stainless steel and 12 are clad with 0.010" type 304 stainless steel clad.

The UO_2 particle size distribution for all 25 rods is as follows:

Tyler Mesh	Weight Per Cent
-6 +8	9.0
-8 +10	9.0
-10 +14	12.0
-14 +20	27.0
-20 +28	23.0
-28 +35	12.0
-35 +48	3.0
-48 +65	2.0
-65 +100	1.0
-100	2.0
	100.0

All rods were swaged from 1/2" O.D. to 0.4" O.D. in four passes. Swaged UO_2 densities range from 92% to 94% of theoretical. Individual fuel rod densities are presented in Table III.

Work will start in April on establishing parameters for single pass cold swaging 8 mil and 10 mil thick stainless steel clad fuel rods.

TABLE III

FUEL ROD DENSITIES IN ASSEMBLY 2S

Rod No.	Clad Thickness, inches		Density, % T.D.
2	0.015		93.3
4	0.015		93.3
5	0.015		93.2
6	0.015		93.0
22	0.015		93.6
23	0.015		93.6
24	0.015		93.4
25	0.015		93.4
27	0.015		93.6
29	0.015		93.8
30	0.015		93.6
31	0.015		93.6
		Avg.	93.5
400	0.010		92.9
416	0.010		92.8
424	0.010		92.6
427	0.010		93.0
430	0.010		92.1
434	0.010		92.8
435	0.010		93.1

Table III (cont'd)

Rod No.	Clad Thickness, inches	Density, % T.D.
437	0.010	93.1
439	0.010	92.7
443	0.010	92.3
455	0.010	92.3
456	0.010	92.6
476	0.010	92.6
	Avg.	92.7

4. HOT SWAGING

One predicted problem in powder-compacted fuel rods is the possible erosion of the UO_2 particles from a defected fuel rod by the reactor coolant. A solution to this problem would be to effect, by some means, sintering of the UO_2 particles. Hot working of the powder-compacted fuel rods is one possible means of eliminating the erosion problem. Sintering of the UO_2 particles should be promoted by the hot working.

Work to date in hot swaging 6" long cold swage fuel rod specimens has demonstrated that 95% dense fuel rods can be achieved. Effort is currently being directed toward investigating the effect of temperature and hot working on clad physical and metallurgical properties. Table IV shows the effect of temperature on the metallurgical structure of the clad.

Table IV
DENSITY AND CLAD CONDITION VS. SWAGING TEMPERATURE

Sample No.	Swaging Temp. (°C)	Rod Density	Clad Condition
1	800	95.2	Sensitized
2	800	94.8	Sensitized
3	900	94.6	Slightly sensitized
4	900	94.6	Slightly sensitized
5	1000	95.8	Good
6	1100	95.3	Large grain size
7	1200	95.3	Large grain size

Adverse metallurgical conditions are encountered in the clad except when swaging at 1000 °C. Six samples were then swaged at 1000 °C to further determine density and clad condition. Densities of the rods were 93.5, 94.9, 95.4, 95.4, 95.4, and 95.6% of theoretical. Clad condition has not yet been determined.

Construction of a furnace has been completed to accommodate heating 36" long fuel rods for hot swaging, or thermal treatments of cold swaged rods. This furnace uses natural gas as a heat source.

Work on induction hot swaging fuel rods has started. An induction coil has been designed to fit immediately in front of the swaging die. Attempts to hot swage 40" long rods filled with MgO were successful. Rods having a starting MgO density of 86% T.D. were increased to 89% to 90% by hot swaging. Design improvements are now underway to allow subsequent work to be done with UO_2 filled rods.

5. SWAGED PELLET FUEL

Loading ground pellets into tubes requires a minimum clad-pellet diametrical gap of 4 mils in order to prevent the pellets from catching or binding inside the tube. Unground pellets would require even a larger gap. Reduction of the pellet-clad gap is desirable both to increase the thermal performance of the fuel rod and to prevent wrinkling of the clad (thin clad) from reactor coolant pressure. A program is underway to investigate swaging using nylon dies as a method of reducing the as-loaded diametrical gap between pellet and clad.

Process parameters have been established for swaging 6-mil and 12-mil thick stainless steel clad fuel rods loaded with simulated unground pellets. Work is currently being conducted on fuel rods with 8-mil and 10-mil thick clad,

ENTRANCE END

EXIT END

FIGURE 19 - CALROD TANDEM ROLLING MILL

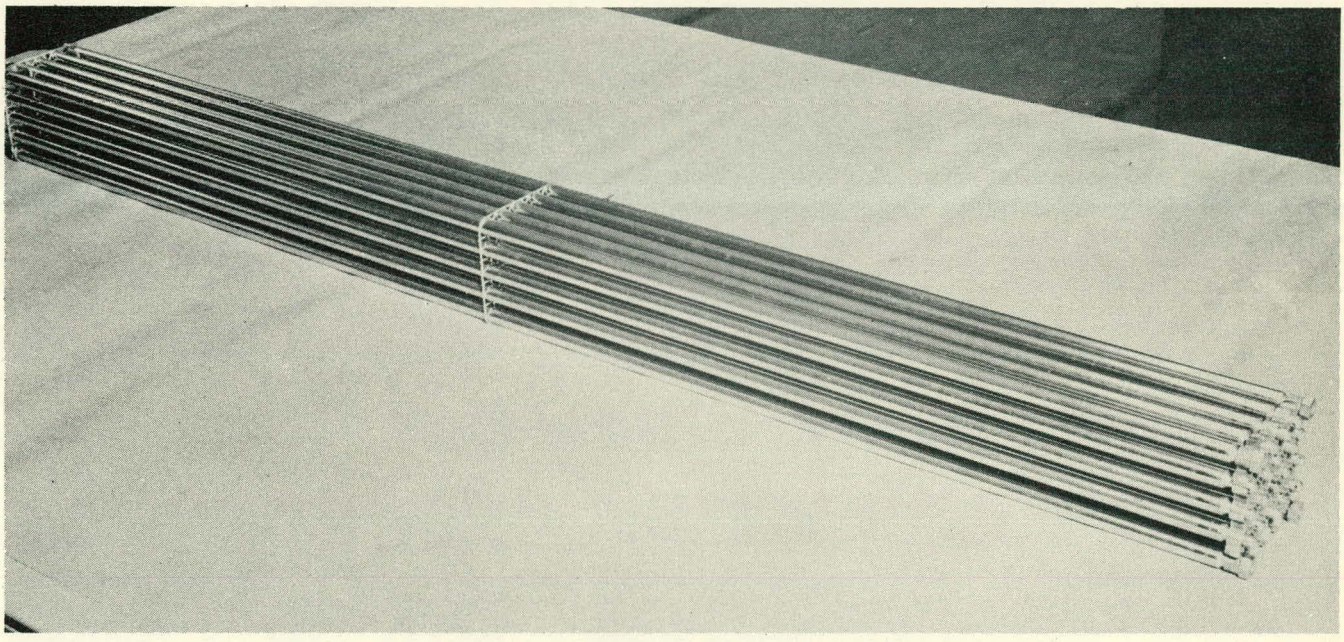

FIGURE 20 - SPECIAL FUEL ASSEMBLY 2S

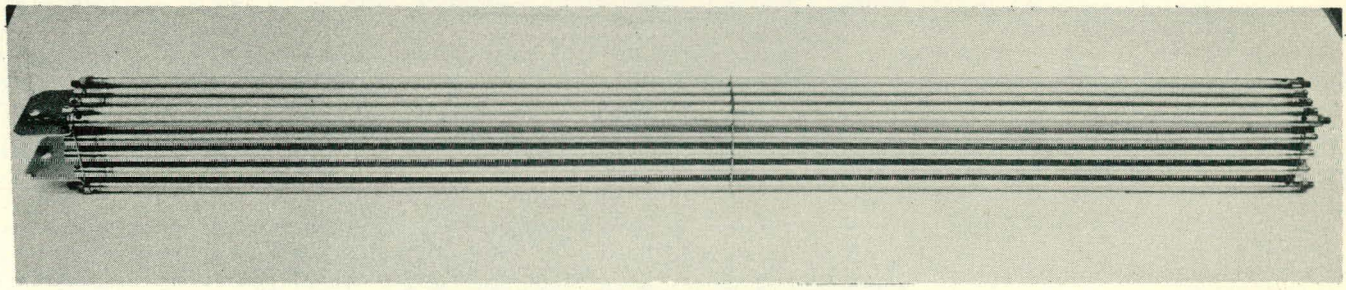

FIGURE 21 - SPECIAL FUEL ASSEMBLY 1S

which will be used for the swaging of assembly 6-S.

Fuel bundle 1-S (Figure 21) was fabricated by swaging over UO_2 pellets which were centerless ground to simulate unground conditions, e.g., ground to a normal frequency distribution between tolerance limits. Thirteen of the rods contain pellets with a diameter tolerance of $\pm$ 0.005" and 12 rods contain pellets with a diameter tolerance of $\pm$0.003". The pellets are clad with 12 mil type 304 stainless steel.

6. PELLET PROCESS IMPROVEMENTS

The effort on reducing pellet fabrication costs by increasing pellet L/D ratio and using a multiple cavity die is in production test stage.

In addition to the above work on reducing pellet fabrication costs, effort of a survey nature was initiated this month evaluating isostatic pressing, explosive forming and hot pressing as techniques for fabricating low cost UO_2 pellets or fuel rods. Facilities for investigating these fabricating processes are available should the survey indicate economic incentives.

"Hydraulic" Pressure Equalizer - A device has been designed to equalize the pressure on the bottom punches when using multi-cavity dies. By this means a more consistent green density should be possible. The device as manufactured uses rubber as the "hydraulic" medium. Tests made with a Universal Testing machine were inadequate to show quantitatively the pressure transmission but indicated no damage to the rubber under 10 tons of applied load. A production test has been written to install the device on one of the production presses during the fabrication of the next production fuel load in the pellet shop.

Increased L/D Pellets - A production test has been formulated to define the

limits of length to diameter ratio which may be approached using the present equipment. The test is scheduled for April.

Hot Pressing - Previous work has indicated that pellets of over 95% density may be hot pressed at around 900 °C. Further work is planned to define cycle time, die wear and pellet chemistry. A press suitable for hot pressing is available in the Laboratory for these tests. A die has been designed and ordered. Die delivery is expected in April.

Isostatic Pressing - A preliminary investigation has shown that good density rods having sufficient green strength for machining may be formed isostatically from pre-granulated ceramic grade UO_2 powder without binder at 20,000 psi. Literature has been requested on automatic types of isostatic presses to determine the feasibility of the method and the production rates which may be expected.

Explosive Forming - Little or no information has been obtained on this relatively new concept of powder compaction. It has been demonstrated that high density compaction is possible but economic application does not appear feasible. Information has been requested from those known to be doing work in this field.

7. EROSION TESTING DEFECTED POWDER COMPACTED FUEL RODS

One conjectured problem in powder compacted fuel rods is the possible erosion of the UO_2 particles from a clad defect (hole or split) in a fuel rod. Erosion flow tests are being conducted on purposely defected powder compacted fuel rod samples to determine the relative "erosion characteristics" of various types of fuel.

Sixteen 3" long defected, powder compacted fuel rod specimens were prepared

for a 1000 hour erosion flow test, which started February 28. Samples of fuel rods made by: 1) cold swaging, 2) hot swaging, and 3) cold swaging followed by a post-swage heat treatment for 1 hour and 1100 °C, are being tested. Each fuel specimen contains a single longitudinal slot, 1/4" to 1" long, 0.020" wide, and deep enough to just break through the clad and expose UO_2. Table V shows the various fuel types being tested and the test conditions:

Table V
EROSION SPECIMEN IDENTIFICATION

Sample No.	Fabrication Method	Slot Length	Position in Loop
1	Hot Swage	1"	535°F water, ~7 fps
2	Cold Swage + Heat Treated	1/2"	535°F water, ~7 fps
3	Cold Swage	1/2"	535°F water, ~7 fps
4	Hot Swage	1/2"	535°F water, ~7 fps
5	Cold Swage + Heat Treated (CaO additive)	1/2"	535°F water, ~7 fps
6	Cold Swage	1/4"	535°F water, ~7 fps
7	Cold Swage + Heat Treated (TiO additive)	1/4"	535°F water, ~7 fps
8	Hot Swage	1/4"	535°F water, ~7 fps
9	Hot Swage	1"	545°F water steam, ~10 fps
10	Cold Swage + Heat Treated	1/2"	545°F steam water, ~10 fps
11	Cold Swage	1/2"	545°F steam water, ~10 fps
12	Hot Swage	1/2"	545°F steam water, ~10 fps
13	Cold Swage + Heat Treated (CaO)	1/2"	545°F steam water, ~10 fps
14	Cold Swage	1/4"	545°F steam water, ~10 fps
15	Cold Swage + Heat Treated (TiO)	1/4"	545°F steam water, ~10 fps
16	Hot Swage	1/4"	545°F steam water, ~10 fps

The 1000 hour test was interrupted March 23, 1961, after 570 hours of continuous flow due to the necessity to shut down the flow loop for reasons

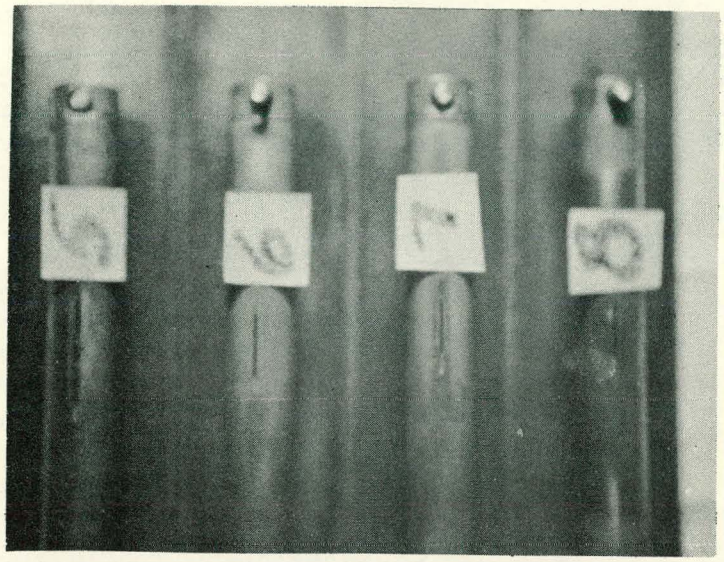

FIGURE 22 - EROSION SAMPLES AFTER 570 HOURS IN 535 o F FLOWING WATER
(SAMPLE NOS. IDENTIFIED IN TABLE V)

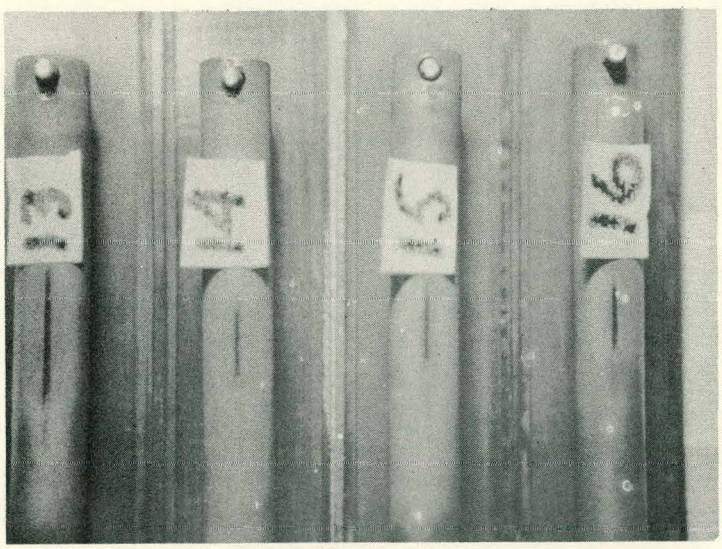

FIGURE 23 - EROSION SAMPLES AFTER 570 HOURS IN 545 ° F FLOWING STEAM AND WATER
(SAMPLE NOS. IDENTIFIED IN TABLE V)

not associated with the test. Eight samples were visually inspected under 20X magnification. These samples are shown in Figures 22 and 23. No significant erosion of UO_2 out of the samples was observed. Time was insufficient to permit weighing the samples. The samples were replaced the same day, and the test is continuing. Scheduled shut down for completion of the 1000 hour test is April 11, 1961. A second 1000 hour test is planned using some of the first 1000 hour test samples plus vibratory compacted samples.

8. VIBRATORY COMPACTED FUEL

Vibratory compaction is receiving considerable attention throughout the country as a method of producing UO_2-filled fuel elements. In the vibratory compaction process, fused UO_2 particles are loaded into a tube and subsequently sonically vibrated to effect dense packing of the UO_2 particles. Vibratory compaction is under investigation using an MB electrodynamic unit to determine techniques and establish parameters required to pack UO_2 to high densities (greater than 90% T.D.)

The primary effort during this period has been to study many binary and ternary systems composed of coarse, medium, and fine particles of UO_2, vibrate these mixtures for precise lengths of time at fixed sonic energies, and then calculate the density achieved for the particular mixture. Although high density is the goal of this work, more emphasis was placed on mapping out the density-composition than in achieving high density. The knowledge gained by these studies will make process control more attainable. Simple three particle size mixes studied are capable of about 83% of theoretical density. "Broad-banded" mixes appear necessary to achieve densities above 90%.

One hundred twenty-five different compositions were vibrated in 0.400" I.D.

Stainless steel tubing in this period covering the range from single particle sizes to broad mixtures, simple binary systems, simple ternary systems, and as-received powder. A brief summary of results follows:

1. Single sieve sizes range from 53% T.D. for +6 material to a maximum of 58% T.D. for 10/14 mesh.
2. Simple binaries range from 47% T.D. for a mixture of 3/6 and 6/8 to 77½% T.D. for one third - 325 with two thirds 10/14.
3. Ternary mixtures yield 75% to 78% T.D. for a large range of particle mixtures and a smaller number of compositions yield over 80%. One small peak occurs at 83% T.D. for 54 w/o of 6/8, 28 w/o of 35/48, and 18 w/o of 270/325. Other ternaries remain to be studied.
4. The same mixture as used by Hanford for 90% T.D. UO_2 packing in 0.505 I.D. tubing was used for 3.5% UO_2 powder and in 0.400" I.D. stainless steel tubing. This mixture yielded 86% T.D. One of our mixtures gave 86.5% T.D. Table VI shows the two mixes.

Table VI
VIBRATORY COMPOSITION DENSITY COMPOSITION

APED (86.5% T.D.)		HAPO (86% T.D.)	
UO_2 Particle Size	Weight Per Cent	UO_2 Particle Size	Weight Per Cent
6/8 mesh	45%	6/10 mesh	55%
8/20 mesh	15%	1/20 mesh	12½%
35/65 mesh	25%	35/65 mesh	12½%
-325 mesh	15%	-200 mesh	20%

These data discussed above are plotted in graphical form as shown in Figures 24, 25, 26, and 27.

Figure 24: Binary mixtures of various mesh sizes added to 10/14 mesh in different proportions showing high specificity and sensitivity to composition.

THEORETICAL DENSITIES OF THE BINARY SYSTEM, 10/14 MESH WITH VARIOUS PERCENTS OF SMALLER SIZE PARTICLES. SPENCER 3.5 % U_{235} ARC-FUSED MATERIAL.

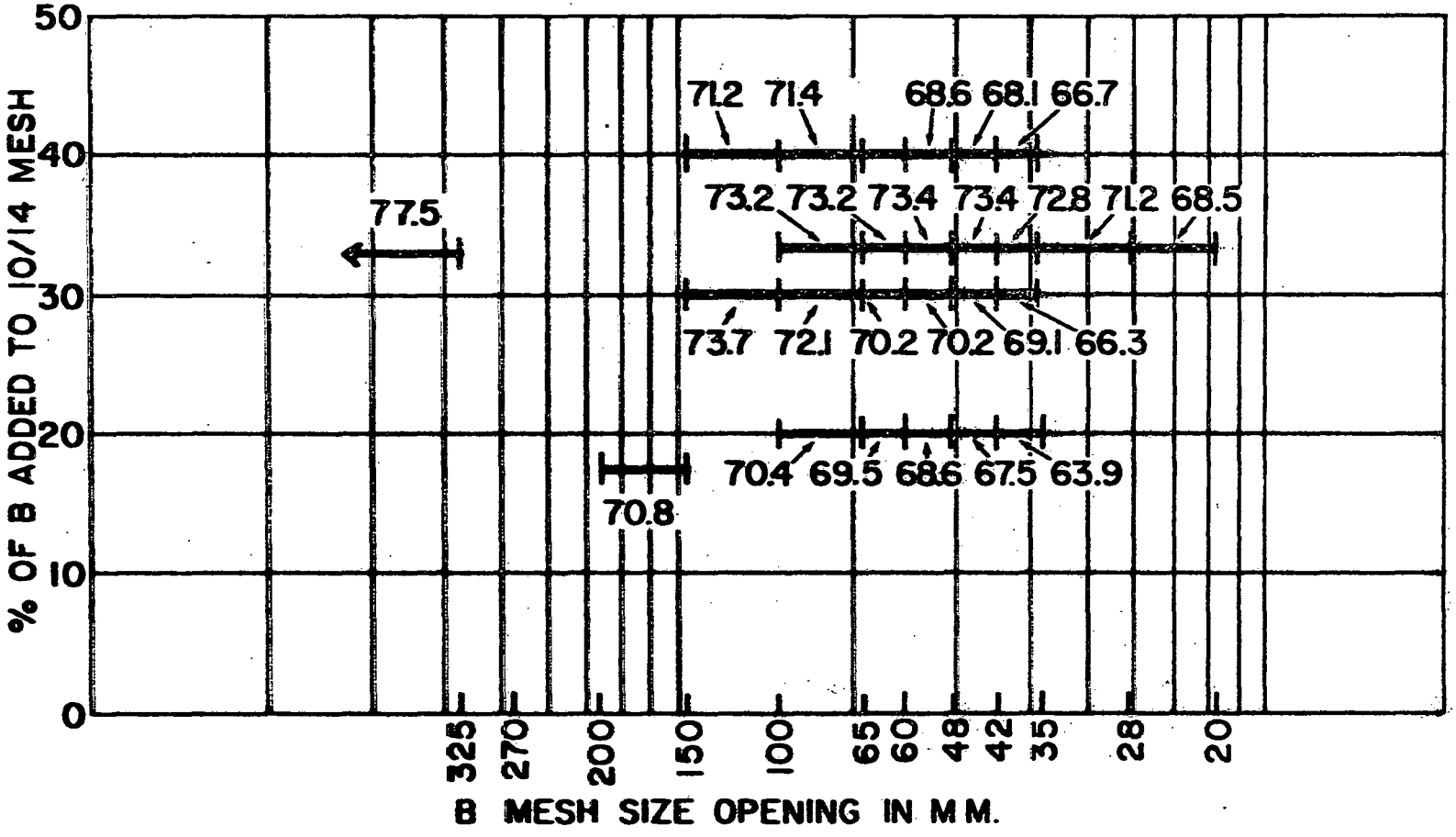

FIGURE 24

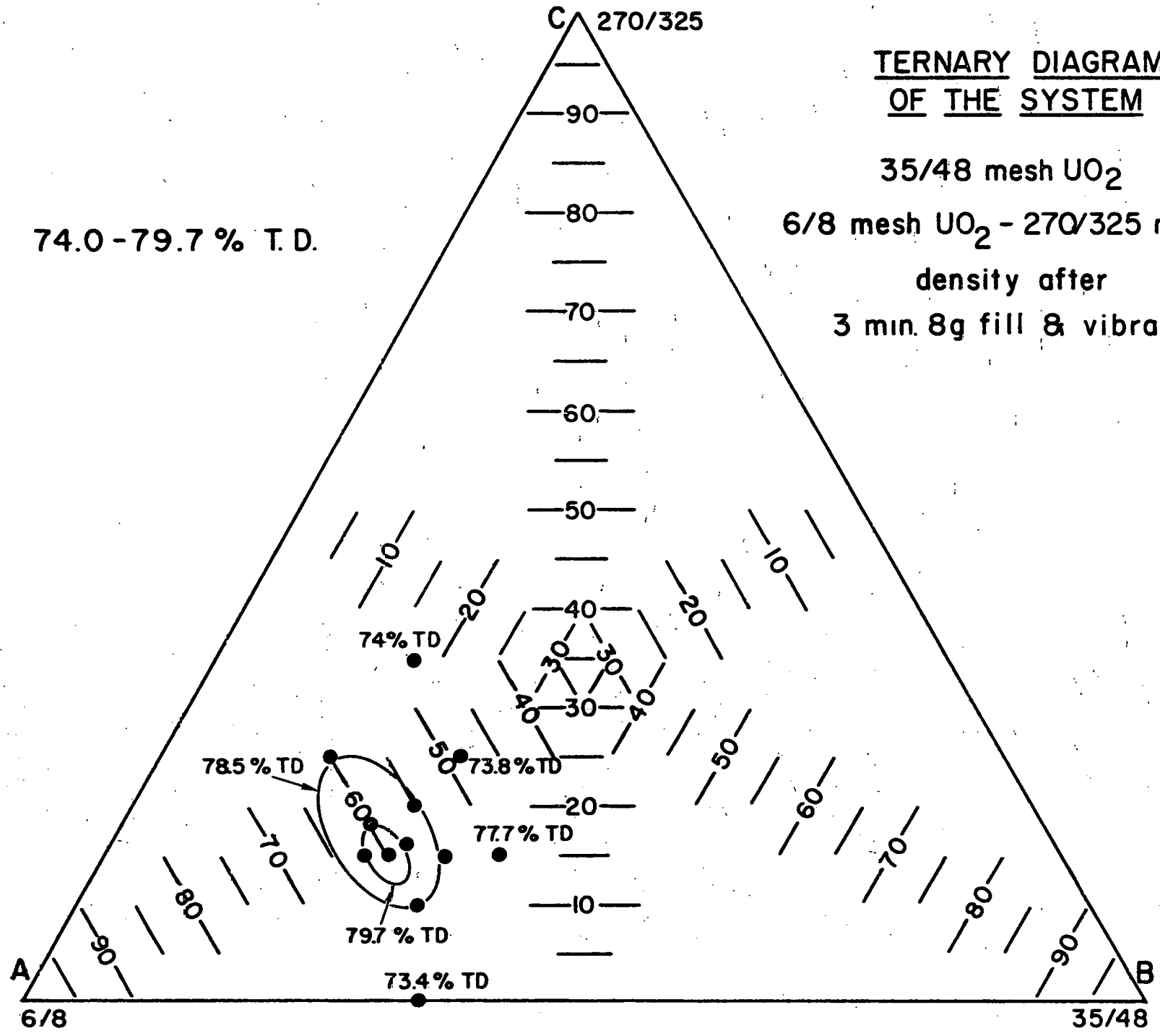

FIGURE 25 TERNARY DIAGRAM OF THE SYSTEM

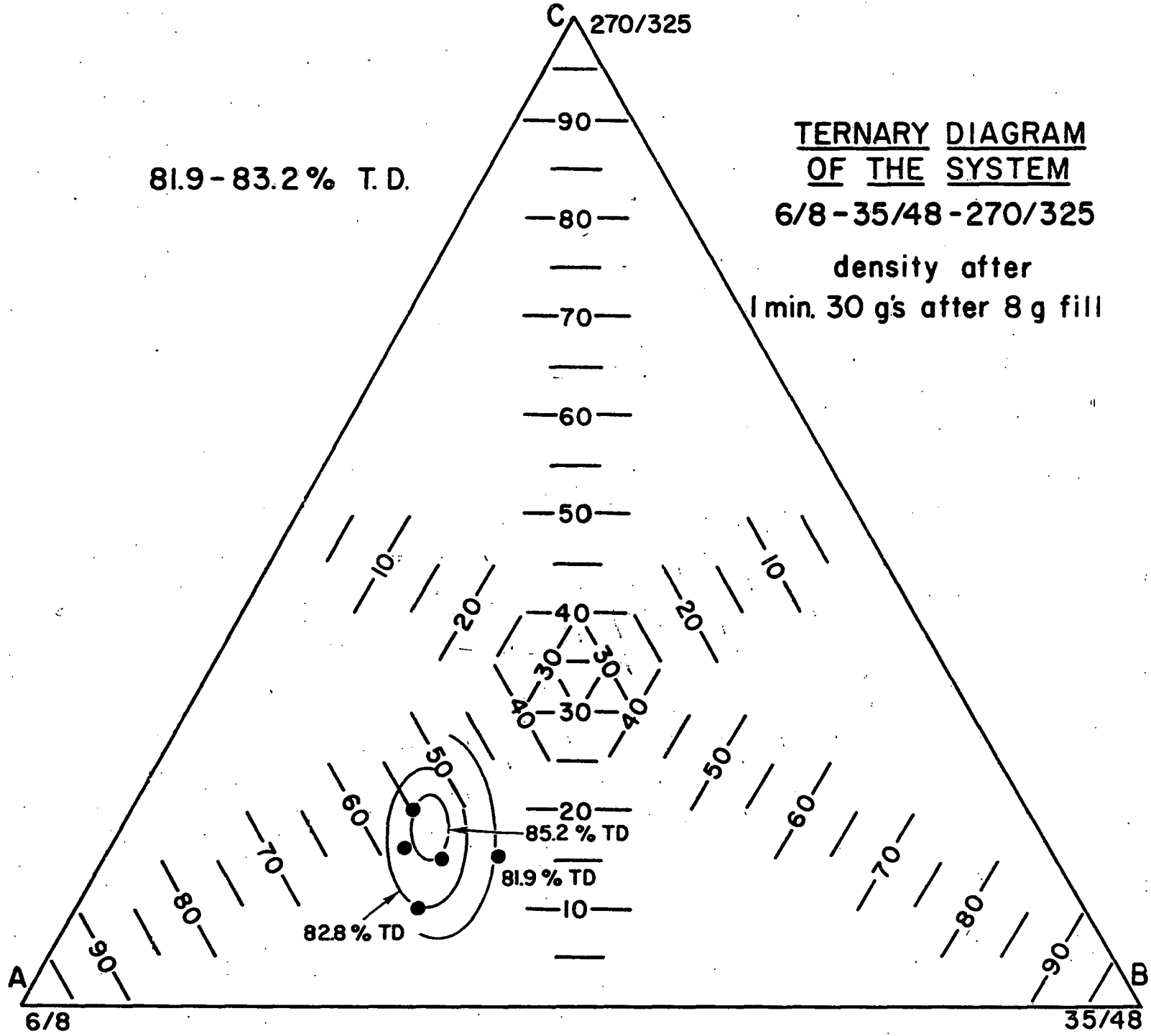

FIGURE 26 TERNARY DIAGRAM OF THE SYSTEM

68.0 - 81.5 % T. D.

Coarse is about equal amounts
of 6/8
8/10
10/14

Medium is equal amounts
35/48
48/65

Fine -200 and about
continuous in
spectrum
200/270
270/325
-325

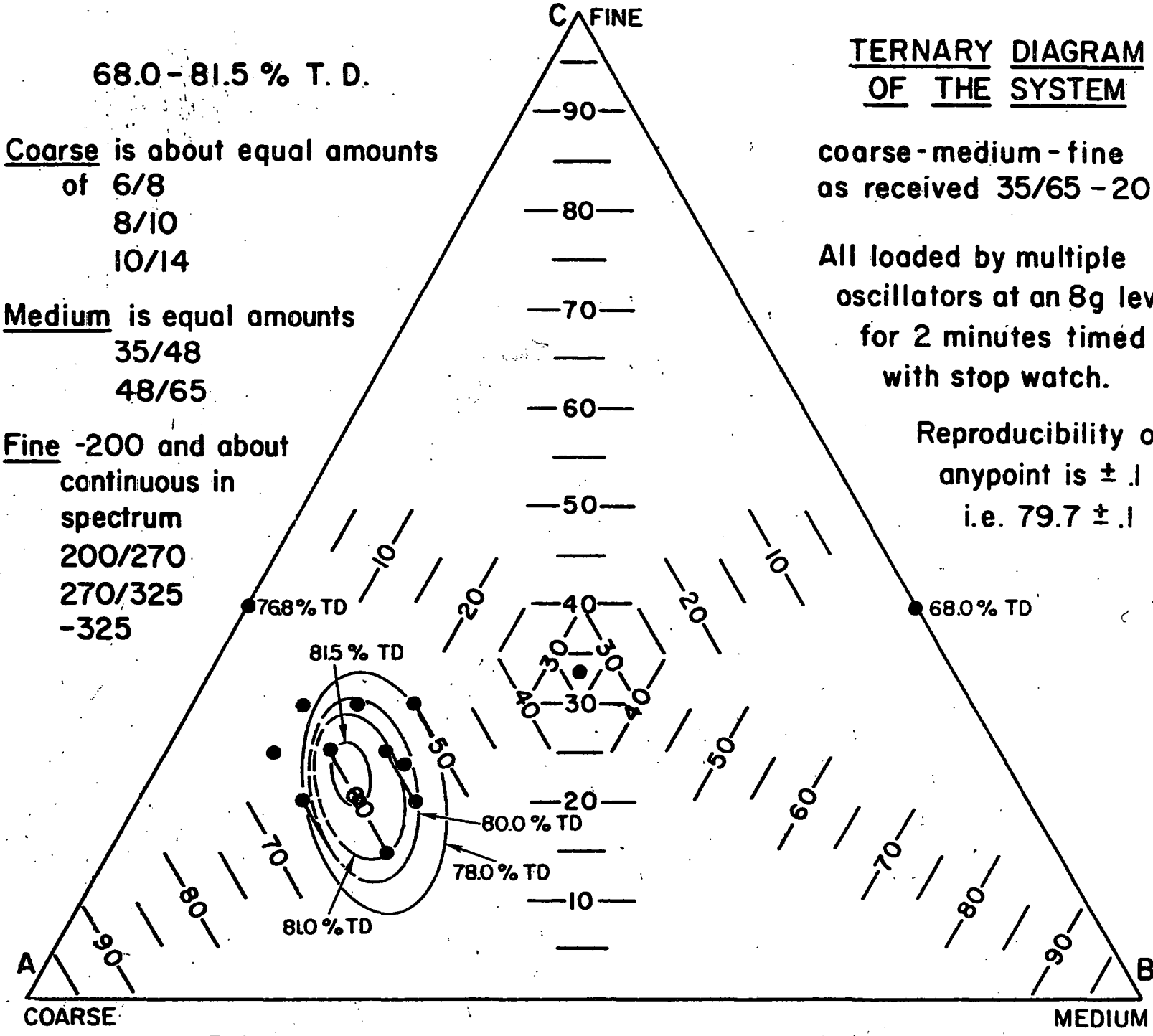

TERNARY DIAGRAM
OF THE SYSTEM

coarse - medium - fine
as received 35/65 - 200

All loaded by multiple
oscillators at an 8g level
for 2 minutes timed
with stop watch.

Reproducibility of
anypoint is ± .1
i.e. 79.7 ± .1

FIGURE 27 TERNARY DIAGRAM OF THE SYSTEM

Figure 25: Ternary plot of narrowly defined coarse, medium and fine, showing densities as packed in a standard 8g, 3 min. fill and vibration.

Figure 26: A few of the same points as above after 1 min. at 30 g's which causes powder attrition and change of composition. Note that the mix which gave highest density as poured under low g without attrition did not necessarily result in the highest density after working. Thus, it is more essential to find that mix which will move to the ultimate composition under vibration.

Figure 27: Ternary plot of a more practical mix actually composed of about 8 or 9 sieve sizes arbitrarily divided into 3 groups of coarse, medium, and fine.

Interest also lies in achieving many mixes which will yield about 85% density, since this is about the level required for one pass swaging. Real difficulty lies in analyzing the results of other than ternary mixtures because of the lack of ways to adequately graph the results and thus guide the direction of motion.

9. MECHANICAL DESIGN

End Plugs - Drawn cup type end plugs have been fabricated in the Equipment Shop at the rate of 100 finished pieces per minute. As a result, economic feasibility of this process is definitely established at less than $0.05 per finished part. Corrosion specimens are still in a BWR environment, but macroscopic inspection after 1000 hours indicated the end plugs and welds were in good condition. Burst tests on drawn cup type end plugs indicate that the cladding is still the limiting item in bursting, thus there is no evidence to date showing that the cup type design is inferior in performance to the more conventional solid type end plug.

VBWR Assemblies - A new fuel bundle design for VBWR special assemblies was initiated and is now complete. This design will be representative of the design being considered for the Consumers Big Rock development assemblies and will allow all of the fuel rods to be removed more easily than any previous designs. In addition, the new design will allow the use of either machined or drawn cup type end plugs and will protect the fuel from potential handling damage, scratching, etc.

Special fuel bundle 4S (helical spacer) has completed its pressure drop testing and results showed approximately a 75% increase in ΔP over the conventional spacer. Since the VBWR operating license requires that an assembly of this type be operated at a burnout margin of 2, until the actual burnout point is determined, the present plan is to use assembly 4S as a prototype of the new fuel design discussed above. This assembly would not then have a helical spacer, however, at the conclusion of an electrically heated burnout test using the helical spacer, the concept will be re-evaluated to determine its suitability for further use.

Completion of VBWR prototype of this new design was accomplished at the end of March. On the basis of results from fabrication of this prototype, design of a Big Rock development fuel assembly will begin in April.

10. SPECIAL VBWR FUEL ASSEMBLIES

The design characteristics of 10 of the 12 Task IB VBWR fuel assemblies has been established, as presented below. Fabrication is in progress on four of these assemblies. The design of the remaining two assemblies will be established by May.

ASSEMBLIES FABRICATED BY THE SWAGED-OVER-PELLET PROCESS

No. 1S

Purpose	To irradiation test marginal and good quality 12-mil thick clad as determined by non-destructive testing with as-sintered pellets.
Clad	0.012" thick 304 stainless
Fuel	3.5% sintered UO_2 ground to an as-sintered distribution.
Rods	Swaged to zero gap. 13 rods to have good quality clad and pellets with 0.010" diameter range. 12 rods to have marginal quality clad and pellets with 0.006" diameter range.
End Plugs	Current standard machined design.
Completion Date	Completed March 17, 1961

No. 4S

Purpose	To irradiation test a mechanical design suitable for Consumers fuel that provides for easy removal of fuel rods.
Clad	0.014" thick 304 stainless
Fuel	4.5% sintered UO_2 ground to 0.003" diameter tolerance.
Rods	Swaged to zero gap.
End Plugs	Current standard machined design.
Completion Date	April 1961

No. 6S

Purpose	To irradiation test 8-mil and 10-mil clad rods fabricated from commercially available material and utilizing a statistical approach to the relaxation of various manufacturing and design variables.
Clad	0.010" and 0.008" thick 304 stainless
Fuel	3.5% sintered UO_2 ground to simulate as-sintered pellets. Forty per cent of pellets $< 94\%$ of the theoretical density; balance of pellets $> 94\%$ dense. Pellets to have varying degrees of chips.
Rods	Swaged to zero gap. 13 rods to have 10-mil clad and 12 rods to have 8-mil clad. Both clad sizes to have nine rods each containing up to 0.002" clad surface defects. Four rods in each clad size to have X-ray rejectable weld defects.

End Plugs	Machined design.
Completion Date	April 1961

ASSEMBLIES FABRICATED BY POWDER COMPACTION BY ROLLING PROCESS

No. 3S

Purpose	To irradiation test fuel rods fabricated by the Calrod tandem rolling process.
Clad	0.015" thick 304 stainless
Fuel	3.5% fused UO_2 (-6 mesh)
Rods	Rolled to 88.5% $\pm$1% density
End Plugs	Collapsible design
Completion Date	April 1961

ASSEMBLIES FABRICATED BY VIBRATORY COMPACTION PROCESS

No. 7S

Purpose	To irradiation test fuel rods fabricated by vibratory compaction to 88% density, minimum.
Clad	0.010" and 0.012" thick 304 stainless
Fuel	4.0% fused UO_2 (-6 mesh, conditioned)
Rods	Vibratory compacted to 88% density, minimum
End Plugs	Current standard machine design
Completion Date	April 1961

No. 9S

Purpose	To irradiation test fuel rods fabricated by vibratory compaction to 90% dense.
Clad	0.010" and 0.003" thick 304 stainless
Fuel	4.0% fused UO_2 (optimized mix)
Rods	Vibratory Compacted to 90% density
End Plugs	Drawn cup design
Completion Date	June 1961

ASSEMBLIES FABRICATED BY THE SWAGED-OVER-POWDER PROCESS

No. 2S

Purpose	To irradiation test fuel rods fabricated by multiple pass, swaged-over-powder process.
Clad	0.015" and 0.010" thick 304 stainless
Fuel	3.5% fused UO_2 (-6 mesh)
Rods	Swaged to 93% $\pm$1% density using multiple pass techniques. 13 rods to have 15-mil clad and 12 rods to have 10-mil clad.
End Plugs	Collapsible design
Completion Date	Completed March 17, 1961

No. 8S

Purpose	To irradiation test fuel rods fabricated by single pass, swaged-over-powder process.
Clad	0.010" thick 304 stainless
Fuel	4.0% fused UO_2 (-6 mesh, conditioned)
Rods	Swaged to 92% $\pm$1% density, using a single swaged pass technique
End Plugs	Collapsible design
Completion Date	May 1961

No. 10S

Purpose	To irradiation test fuel rods fabricated by cold swaging and vibratory composition, followed by hot working or heat treatment.
Clad	0.010" thick 304 stainless
Fuel	4.0% fused UO_2
Completion Date	June 1961

DEFECTIVE FUEL ROD ASSEMBLY (one only)

No. 5S

Purpose	To irradiation test purposely defective fuel rods fabricated by the four fabrication processes under investigation; and

	certain other special features such as 6-mil cladding, and warm press pellets.
Clad	Varying, depending upon fuel rod, from 6-mil to 17-mil
Fuel	Pellets and fused powder
Completion Date	May 1961

11. MECHANICAL VIBRATION TESTS

Initial vibration tests have been completed on a 36 rod, full scale, Consumers element at reactor conditions. Vibration was detected by strain gages that were mounted 90 degrees apart on the inside surface of the UO_2 pellet filled clad. Two normal rods were instrumented at an axial location of 5/8 of a rod length above the element base. Figure 28 shows the top end of the instrumented element and emerging lead wire carriers. A series of tests were performed with two different spacer arrangements.

General Results

Tests employing the spacer arrangement of the first core design revealed that maximum spanwise deflections of the normal rods were less than .001 inches at all test conditions including the design mass velocity and 10% quality at 1000 psia. The vibration problem for the first core is therefore less than was estimated. Vibration amplitudes as high as .007 inches were measured within a 55 inch span, which is three first core span lengths.

Method

The four strain gage pairs for indicating two dimensional lateral deflections in both instrumented fuel rods were calibrated by applying static point loads to the instrumented span, which was supported by simulated woven-wire spacers. The calibration apparatus and strain recording equipment are shown in Figure 29. The calibration deflections were then converted to the inertial loading case. Corrections for temperature effects and non-uniformities resulting from instrumentation were applied to the data.

Test I Results

For Tests I, three double layer, woven-wire spacers supported the rods in four equal spans and vibration amplitudes were sensed at the center of the third span from the element base. This spacing arrangement is that of the present core design.

Test conditions were at mass velocities of $.7 \times 10^6$ to 1.7×10^6 lb/hr-ft^2 of subcooled water and 0, 5, 10, and 15% quality at 1000 psia. These conditions include those of the reactor design.

The background noise level (60 cps) was equivalent to span vibration amplitudes of .0005 to .001 inches between supports. Lateral vibrations of the instrumented span of this order of amplitude or greater would occur at a frequency of about 49 cps. No vibration could be detected with this sensitivity at any of the conditions. Therefore, fuel rod vibration between the three spacers is less than .001 inch amplitude for reactor conditions. The gage location was not suitable for detecting overall rod length vibrations within spacers.

Test II Results

For Tests II, the upper two spacers of Tests I were removed while the position of the lowest spacer was not changed.

Four tests of an exploratory nature were performed with the un-symmetrical spacer arrangement. Lateral vibrations occurred in the long span at frequencies between 7.1 and 7.4 cps. Rotational frequencies were near 0.2 cps. The vibration was of nearly constant non-directional amplitude for a given set of conditions. The amplitude in the sensor directions varied at the rotational frequency. The amplitudes of vibration are shown below with test conditions:

Test	Pressure (psia)	Mass Velocity (lb/hr ft^2)	Water Temperature (^oF)	Quality	Vibration Amplitude (inches)
A	85	$.7 \times 10^6$	70	---	.002
B	1000	$.7 \times 10^6$	Sat.	.15	.005
C	1000	1.2×10^6	Sat.	.016	.004
D	1000	1.2×10^6	Sat.	.05	.007

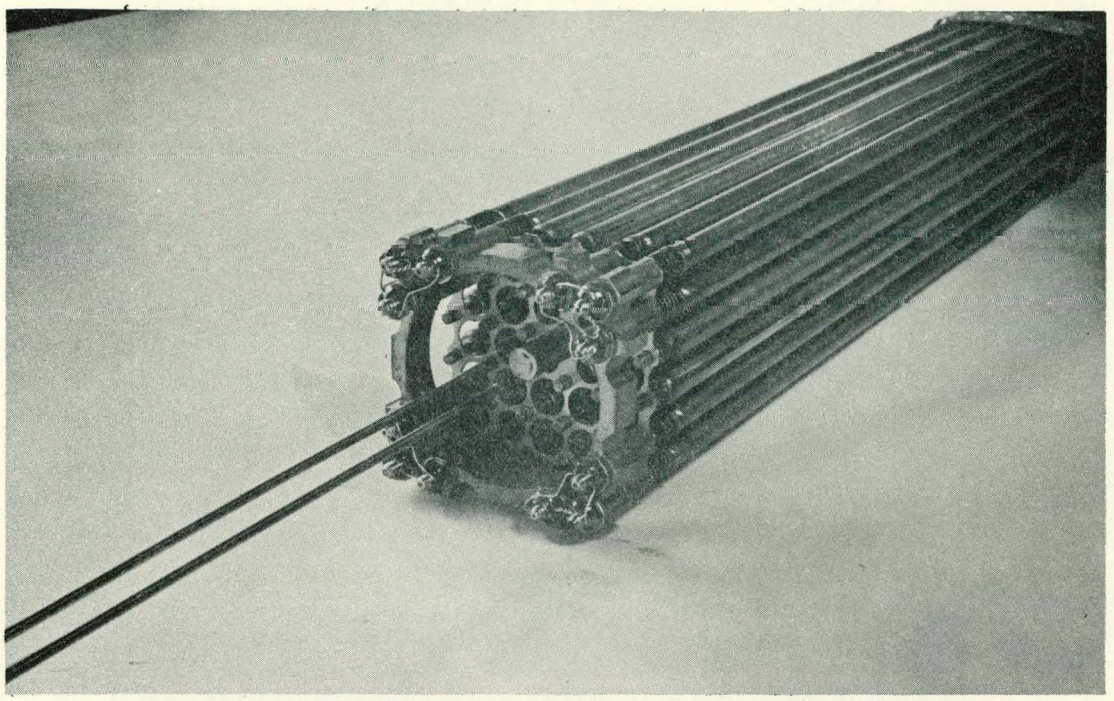

FIGURE 28 - INSTRUMENTED ELEMENT FOR VIBRATION TESTS

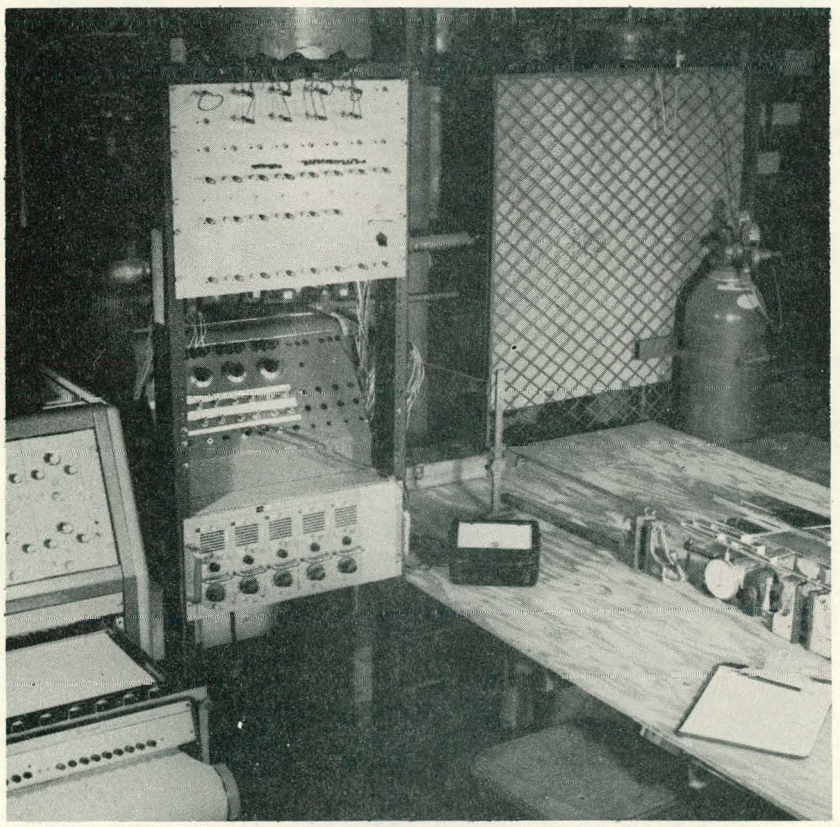

FIGURE 29 - CALIBRATION APPARATUS AND RECORDING EQUIPMENT FOR VIBRATION TESTS

TASK II - STABILITY, HEAT TRANSFER, AND FLUID FLOW

1. TASK OBJECTIVE

Hydrodynamic, thermodynamic, and nuclear effects on reactor performance and stability are to be evaluated analytically and also experimentally in the Consumers Big Rock Reactor. Assurance of reactor stability under conditions of R&D testing is an objective of the program, as is the use of these results and methods to evaluate performance of the 300 MWe HPD conceptual design.

Out-of-pile heat transfer and fluid flow development testing will obtain data in such critical areas as:

a. Burnout heat transfer

b. Pressure drop (single and two-phase flow)

c. Hydraulic stability (forced and natural circulation)

A wide range of operational and design parameters will be evaluated.

2. STABILITY ANALYSIS

An analytical model was conceived to evaluate the hydrodynamic and nuclear stability characteristics of the Consumers Big Rock core and nuclear steam supply system. It incorporates an analytical representation of reactor kinetics, hydrodynamic flow characteristics, including two-phase effects, and thermodynamics effects due to load and subcooling changes. It is believed that the performance of high power density boiling water reactors will be determined, in large measure, by the flow behavior of the two-phase nuclear steam supply system. For this reason particular emphasis was placed on developing what is considered to be an accurate and comprehensive analysis of forced circulation two-phase flow dynamics.

The reactor kinetics and hydrodynamics portions of the analytical model were applied to the 50 MWe Consumers Big Rock plant at rated conditions and were found to predict stable performance comparable to industrial system design criteria. The thermodynamic effects due to load and subcooling changes are yet to be investigated.

The Analytical Model

The analytical model to evaluate the hydrodynamic and nuclear stability characteristics of the Consumers core and nuclear steam supply system is presented in block diagram form in Figure 30. The logic of the model consists of analytical representations of physical phenomena. These representations, or transfer functions, are transformed from basic defining differential equations and describe the linearized phase and magnitude relationships between two variables (output and input) as a function of frequency. The various transfer functions employed in the analytical model are shown diagrammatically in Figure 30 as boxes in the flow logic paths. The following are brief descriptions of the analytical representations used in the stability model.

Reactor Kinetics

A single delay group - linear representation of the thermal fission (Neutron density-N*) of slightly enriched U-235 as a result of excess reactivity (Δk).

Doppler

A linear representation of the regenerative effect on excess reactivity owing to a change in average fuel temperature which in this model is related to neutron density (N*).

Fuel Model

A linear transformation of the thermal diffusion equation which relates the heat imparted to the fluid at the surface of the fuel element (Q*) to the neutron density (N*).

Pressure Rate

A linear relationship which describes the time rate of pressure change in the nuclear steam supply system (P*) with respect to the energy balance of steam flow rate and enthalpy ($W_g h_g$*), reactor heat (Q*), and feedwater flow rate and enthalpy ($W_{FW} h_{FW}$*).

Saturation and Subcooling

A linear representation which relates pressure rate effects ($\dot{P}$*) to the energy ($W_T \Delta h_s$*) which must be supplied by the core to overcome inlet subcooling. Effects of feedwater temperature variations are also illustrated through the enthalpy h_{FW}*.

Pressure Voids

A linear relationship which describes the steam volume within the core (Up*) as a function of the time rate of pressure change in the nuclear steam supply system ($\dot{P}$*). This is the flashing type phenomenon.

Pressure Reactivity

A linear relationship which describes the excess reactivity (Δk_p) due to steam volume changes (U_p*) within the core that are caused by pressure variations. This is a transport relation which averages the steam volume due to flashing within the core and assigns a void worth of reactivity to that average.

The Hydrodynamic Analysis

The hydrodynamic portion of the analytical model is the distinguishing feature of this stability analysis. It is based upon the physical concepts of momentum interchange, conservation of energy, and continuity of mass and does not rely in any way upon correlations or assumed relationships. It is a system of six transient equations which describe the mechanics and thermodynamics of two-phase flow loops. The independent variables of the hydrodynamic model include: heat input to the fluid and subcooling of the single phase inlet fluid to the heater; the dependent variables include: single-phase inlet

fluid velocity, two-phase pressure drop, steam velocity in the two-phase flow region, water velocity in the two-phase flow region and steam volume fraction in the two-phase region. The only dependent variable needed for this stability analysis, however, is the steam volume fraction U_{Qh}* (see Figure 30). This hydrodynamic model has been described in detail and verified experimentally for both steady-state and transient natural circulation problems.(1)

It was necessary for the purposes of this stability analysis to further develop the hydrodynamic model so that:

(a) It would accept forced circulation flow problems,

(b) The rather involved mathematical solutions could be reduced to a linearized transfer function acceptable for a frequency-phase shift analysis (Bodé analysis),

(c) Solutions could be readily obtained.

All three of the foregoing development points were completed during the past quarter and are manifested in the modified digital computer code 5-VLOP.

It should be noted that the hydrodynamic model can be applied to the stability analysis in two ways:

(a) Loop hydrodynamics - the reactor core, two-phase flow region and recirculation loop is investigated for its feedback contribution to system stability, and

(b) Parallel flow channel hydrodynamics - a single hot channel within the reactor core is investigated for its performance in parallel with the rest of the core for flux noise predictions. Individual channels within the reactor core operating in a parallel flow channel arrangement can be appreciably more underdamped than the whole or lumped core and still not adversely affect reactor stability. They will, however, contribute

(1) Beckjord, E.S., "The Stability of Two-Phase Flow Loops and Response to Ships Motion," GEAP 3493.

significantly to operating flux noise by permitting disturbances in the radial and axial flux distribution to be perpetuated.

The heat-subcooling reactivity transfer function of the stability analysis is similar to the pressure reactivity model already described. The two are similar in that both relationships describe excess reactivity as a function of steam volume. They differ, however, owing to the fact that heat and subcooling generate steam volume in a manner quite unlike flashing.

Reactor - Recirculation Loop Performance

The reactor kinetics, fuel model, loop hydrodynamics and heat-subcooling reactivity can be combined to form a reactor-recirculation loop. An analysis of this segment of the stability model for the Consumers 50 MW core at rated operating conditions was accomplished during the last quarter. A diagram of this portion of the stability model and the transfer functions used is presented in Figure 31. Notice the path in the hydrodynamic model which is applied to analyze the parallel channel noise as an open loop disturbance.

The reactor kinetics, fuel, loop hydrodynamics and heat-subcooling reactivity transfer functions were investigated by the use of a frequency analysis (Bodé analysis) and reduced to a single closed loop transfer function which will be employed in the entire stability model of Figure 30. The frequency response plot of the loop hydrodynamics and heat-subcooling reactivity feedback network ($\Delta K_Q/Q^*$) for the 50 MW core at rated condition is shown in Figure 32. The open loop stability plot ($\Delta K_Q/\Delta K$) of reactor kinetics, fuel, flow loop hydrodynamics, and heat-subcooling reactivity is presented in Figure 33. It can be seen from this illustration that the

FIGURE 30
CONSUMER'S BIG ROCK STABILITY ANALYSIS
BLOCK DIAGRAM

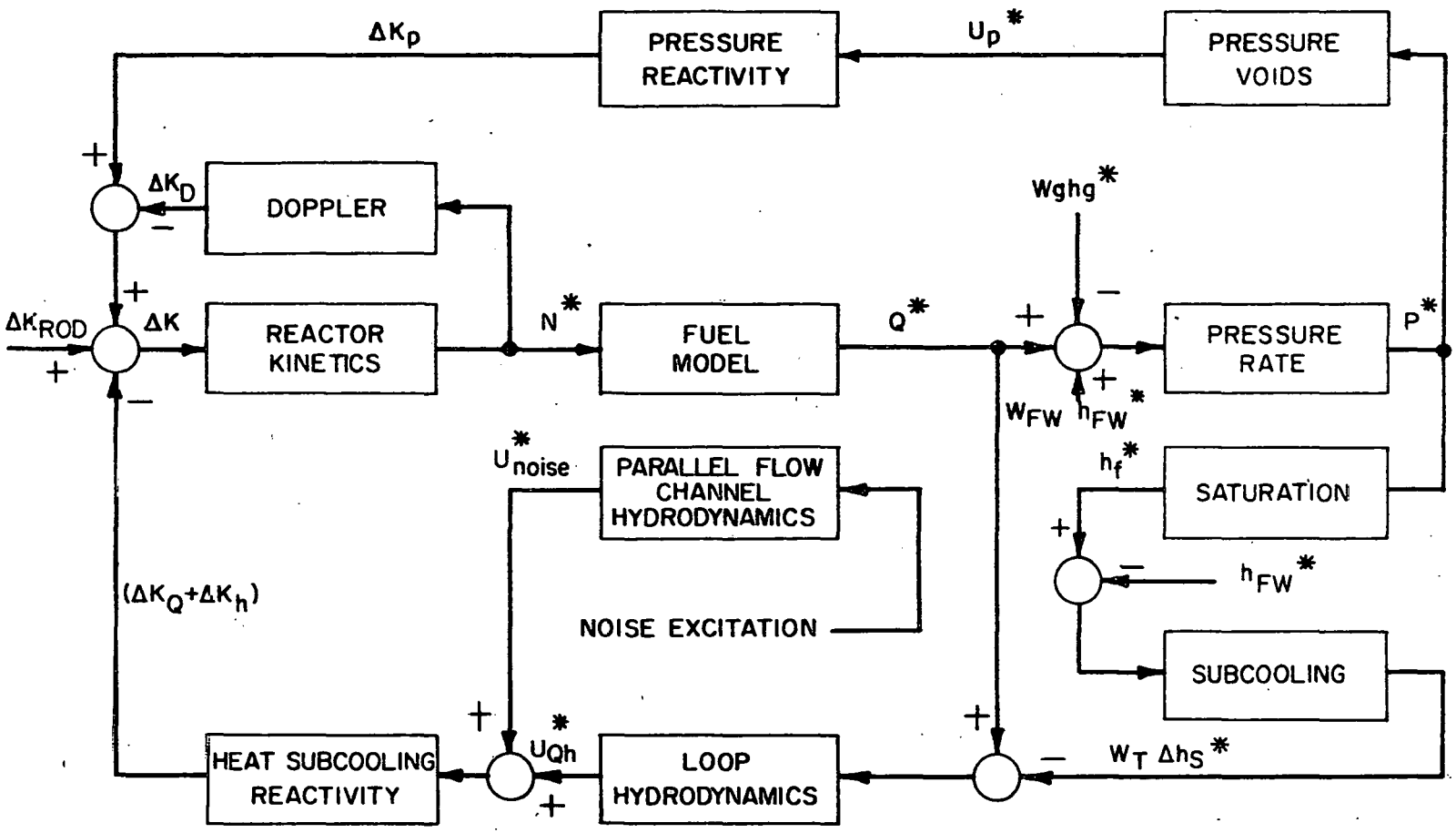

FIGURE 31
REACTOR-RECIRCULATION LOOP BLOCK DIAGRAM
RATED 50 MW OPERATION

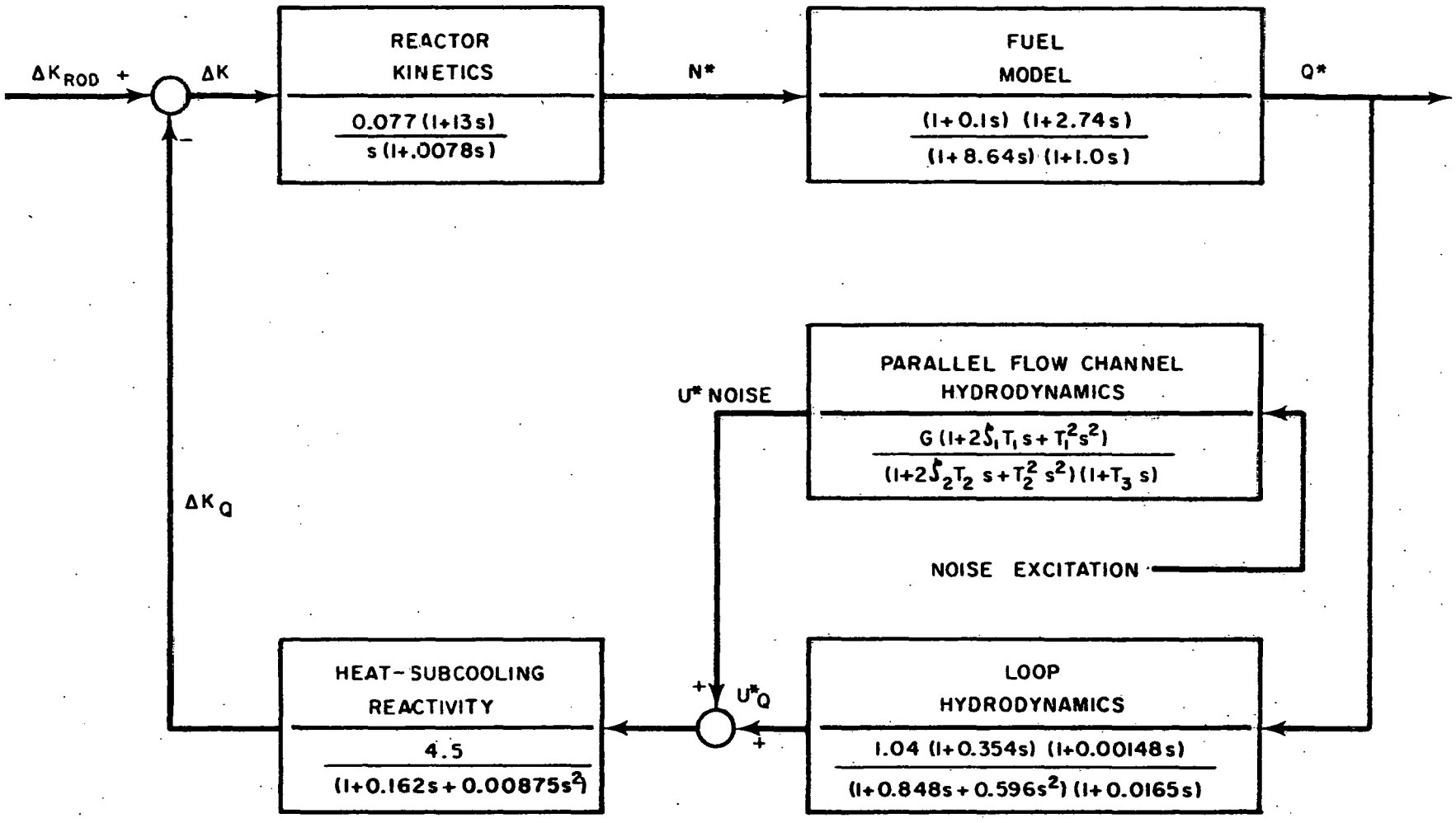

FIGURE 32

FREQUENCY RESPONSE CHARACTERISTIC OF THE FLOW LOOP HYDRODYNAMICS — $\frac{\Delta K_e}{Q^*}$

RATED CONDITIONS
50 MW CORE
VOID WORTH — $ 4.50

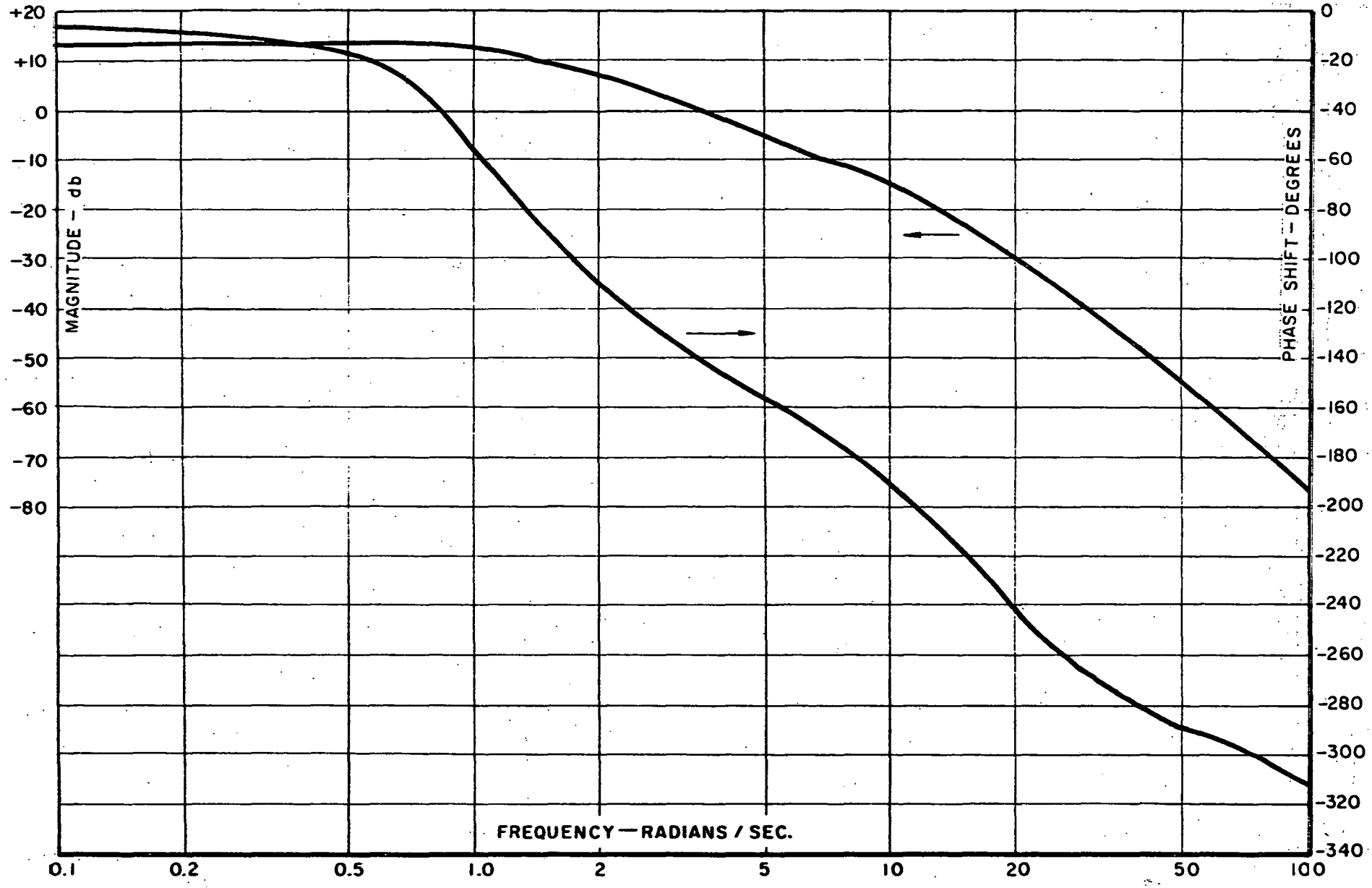

FIGURE 33

FREQUENCY RESPONSE CHARACTERISTIC OF THE REACTOR-RECIRCULATION LOOP — $\frac{\Delta K_e}{\Delta K}$ (OPEN LOOP)

RATED CONDITIONS
50 MW CORE
VOID WORTH — $ 4.50

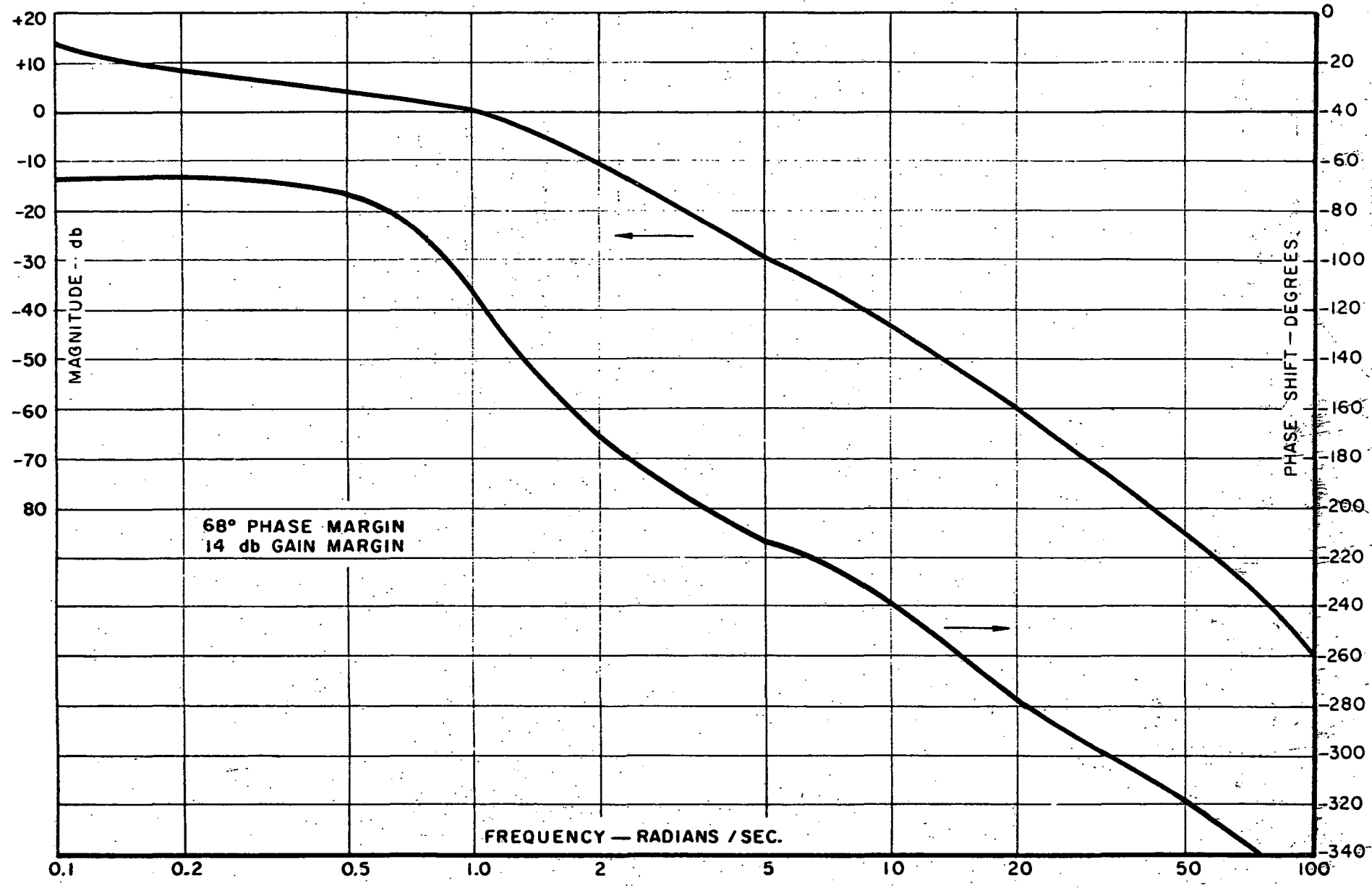

FIGURE 34

FREQUENCY RESPONSE CHARACTERISTIC OF THE REACTOR-RECIRCULATION LOOP- $\frac{Q^*}{\Delta K_{ROD}}$ (CLOSED LOOP)

RATED CONDITIONS
50 MW CORE
VOID WORTH — $ 4.50

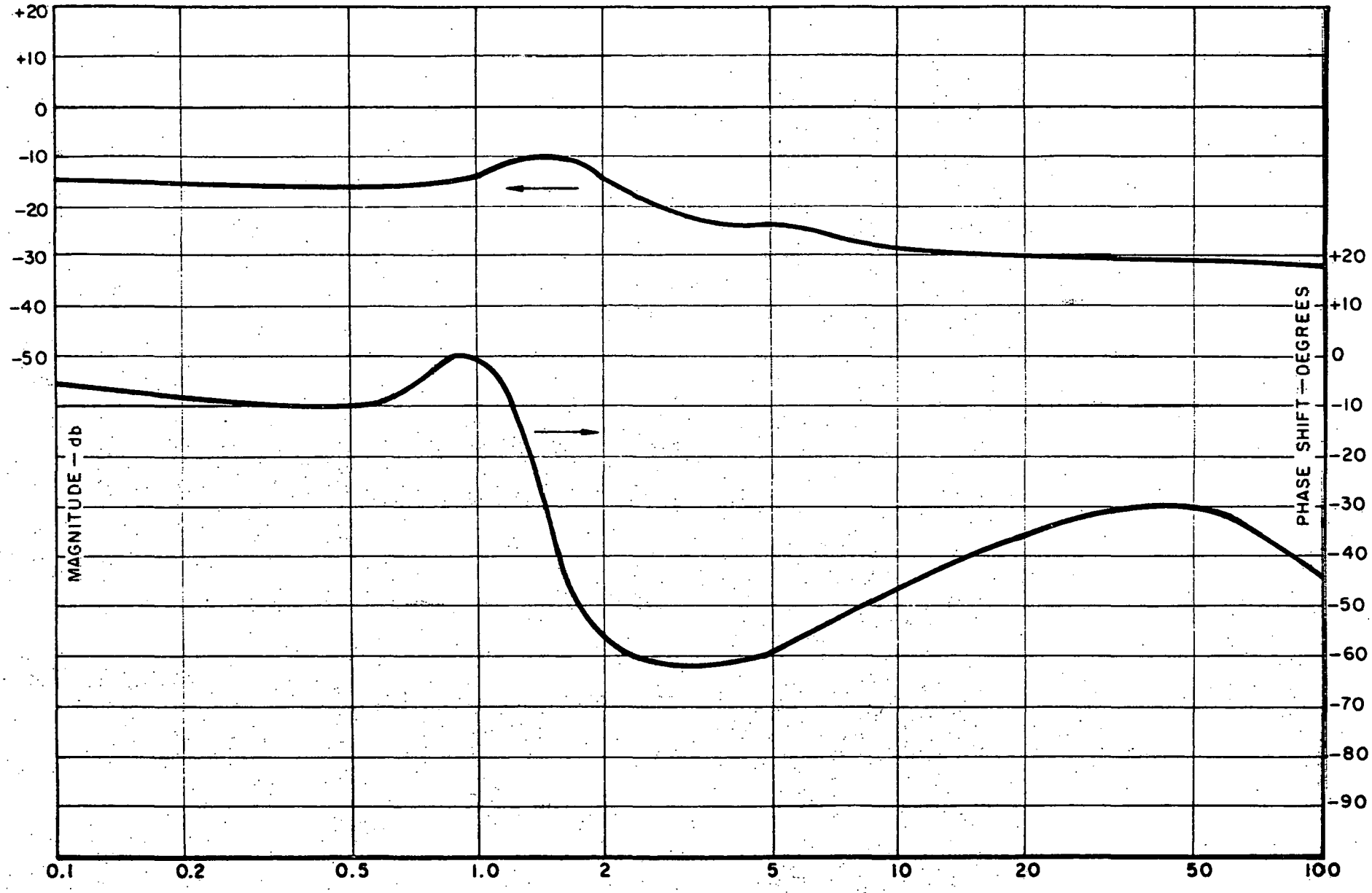

reactor-recirculation loop is stable with 68° phase margin and 14 db gain margin, which compares favorably with conventional feedback system design criteria. The closed loop performance of the network ($Q^*/\Delta K_{rod}$) is shown in Figure 34. It should be pointed out that the hand-calculated Bodé analysis of the reactor-recirculation loop was performed concurrently with an analog computer study. Results of both analyses were checked against each other and found to yield identical results.

The closed loop performance of the reactor-recirculation flow loop shown in Figure 34 is presently being studied in conjunction with the pressure related feedback response for system stability of the 50 MW core at rated conditions (see Figure 30). The parallel flow channel contribution to expected operating flux noise will be studied immediately thereafter.

3. AIR-WATER FLOW TESTS

Preliminary testing of a 1/5 scale Consumers Big Rock flow model established the need for a baffle in the reactor vessel. A series of plates located immediately above the riser inlet was tested to establish a controllable water level in the vessel. Evaluation of high speed movies taken of each baffle plate determined that a flat plate with an octogonal shaped hole to permit fuel handling in the core without removal of the baffle plate was the most satisfactory.

The asymmetrical riser configuration introduced a vortex in the back side of the vessel between the two end risers. As a result of this vortex, "slugging" of the two phase mixture in the end risers resulted. Various combinations of horizontal and vertical plates were installed to destroy this vortex and insure uniform flow distribution to all risers with a minimum of slugging.

High speed movies were taken of all configurations and results are being

evaluated. Preparation of the final test results and report is in progress. Movies showing the phases of the testing will be made available to augment the report.

4. HEAT TRANSFER TEST

Design details of the 9 rod burnout test section and heaters were covered in the last quarterly report. During this quarter detail drawings were completed, bids obtained, and a contract awarded to the Roscoe Kent Mfg. Co. The contract includes furnishing of all materials and manufacture of the burnout test section, and materials and manufacture for modification of an existing test section into the heaters.

All materials have been procured for the test section and heaters. Manufacturing is estimated at 75 per cent of completion and is expected to be completed early in the next quarter.

TASK III - PHYSICS DEVELOPMENT

1. TASK OBJECTIVE

Long fuel lifetime and economically yet effective reactor control is the objective of physics control studies, one of four major areas of study in this task.

A second area is the study of hot spot reduction by power flattening. This will influence the degree of high power density that can be achieved within heat transfer limitations.

A Large High Power Density conceptual design study is to be carried out, and results of the Consumers Big Rock testing will be utilized and applied in the 300 MWe conceptual design evaluation.

The optimizing and scheduling of control is the objective of a computer and data-logging system which is to be studied for feasibility, designed, installed, and operated in conjunction with the Consumers Big Rock Plant.

2. EFFECTS OF BURNUP ON LOCAL POWER DISTRIBUTION

The extent to which enrichment variation can effectively be used to produce local improvements in the power distribution is being investigated.

Calculations were described in the previous quarterly report[2] in which the local fuel bundle peak to average ratio was reduced from 1.28 to 1.05 by employing a variation in fuel rod enrichments. The local power peaking in the fuel bundle results from the water gap between adjacent fuel bundles. This power peak can be decreased by reductions in enrichment in

---

(2) Holland, L.K., "Third Quarterly Progress Report, October - December 1960" GEAP 3632.

fuel rods near the water gap and increases in enrichment in fuel rods away from the gap. The previous analyses have been extended to include the effects of burnup on the local power distribution in an initially power flattened fuel bundle. Two conditions have been investigated; one in which control rod perturbations do not exist and a second in which a control rod initially adjacent to one side of the fuel bundle was withdrawn after approximately one-third of the fuel bundle's life. The results indicate a relatively small increase in the local peaking factor with time when there is no strong control rod perturbation. The effect of a previously inserted control blade was found to produce a local peak to average power ratio about 10% greater than the case without control rods. These calculations were based on a one-dimensional slab geometry and an average enrichment of about 3.5%. It might be expected that including the geometrical effects of a cruciform blade would increase the control blade effect on power distribution. In addition, reductions in enrichment could increase the power perturbations resulting from burnup.

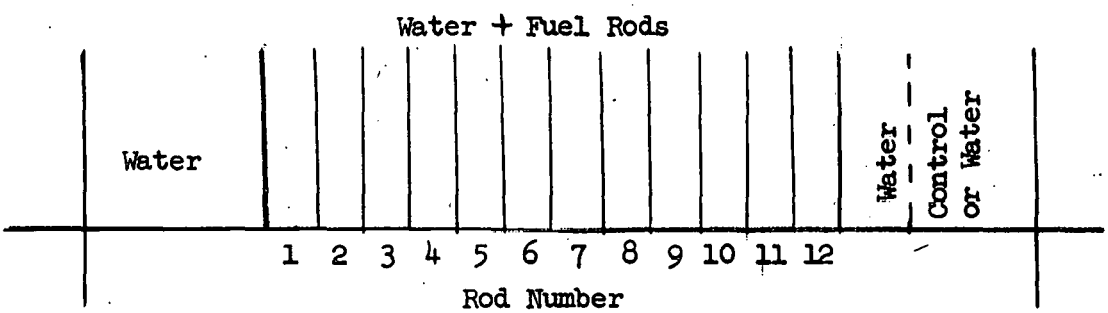

The numbers refer to the twelve rows of fuel rods in a bundle. For the case with no control rods, there is symmetry about the center of the bundle. Figure 35 shows the power produced in the separate fuel rods as

a function of average bundle exposure (MWD/T). It can be seen that the #1 rod adjacent to the water gap initially increases in power and then levels out. This initial rise is attributed to the relatively greater increase in fission cross section in the rods with lower enrichment and greater plutonium buildup. This effect can be seen in Figure 36 where the PU-239 concentration is plotted as a function of exposure for the inner (#6) and outer (#1) rods. As burnup of plutonium becomes significant, the plutonium concentration of the rod adjacent to the water gap falls below that in the central rod. This contributes to the leveling out of the power peak with time. From Figure 35 it can be seen that the initial peaking factor of 1.04 increases to about 1.06 at approximately 7,000 MWD/T and then slowly falls. In this particular case, the power peak shifted from the #3 rod to the #1 rod early in life.

Unfortunately, not all fuel elements in the reactor operate without the perturbing influence of adjacent control blades. In order to study the effect of a control sheet on the local power distribution, the calculation was repeated for the condition in which a control sheet was inserted adjacent to the #12 fuel rod and then withdrawn after an average bundle exposure of 5,000 MWD/T. Figure 37 shows the relative power for several fuel rods in the bundle as a function of exposure. The effect of the control sheet is to reduce the power in the #12 rod to about one-half of the bundle average. After the control sheet is withdrawn, this rod produces the peak power of 1.175 times the average value. Thus, the shielding effect of the control blade has

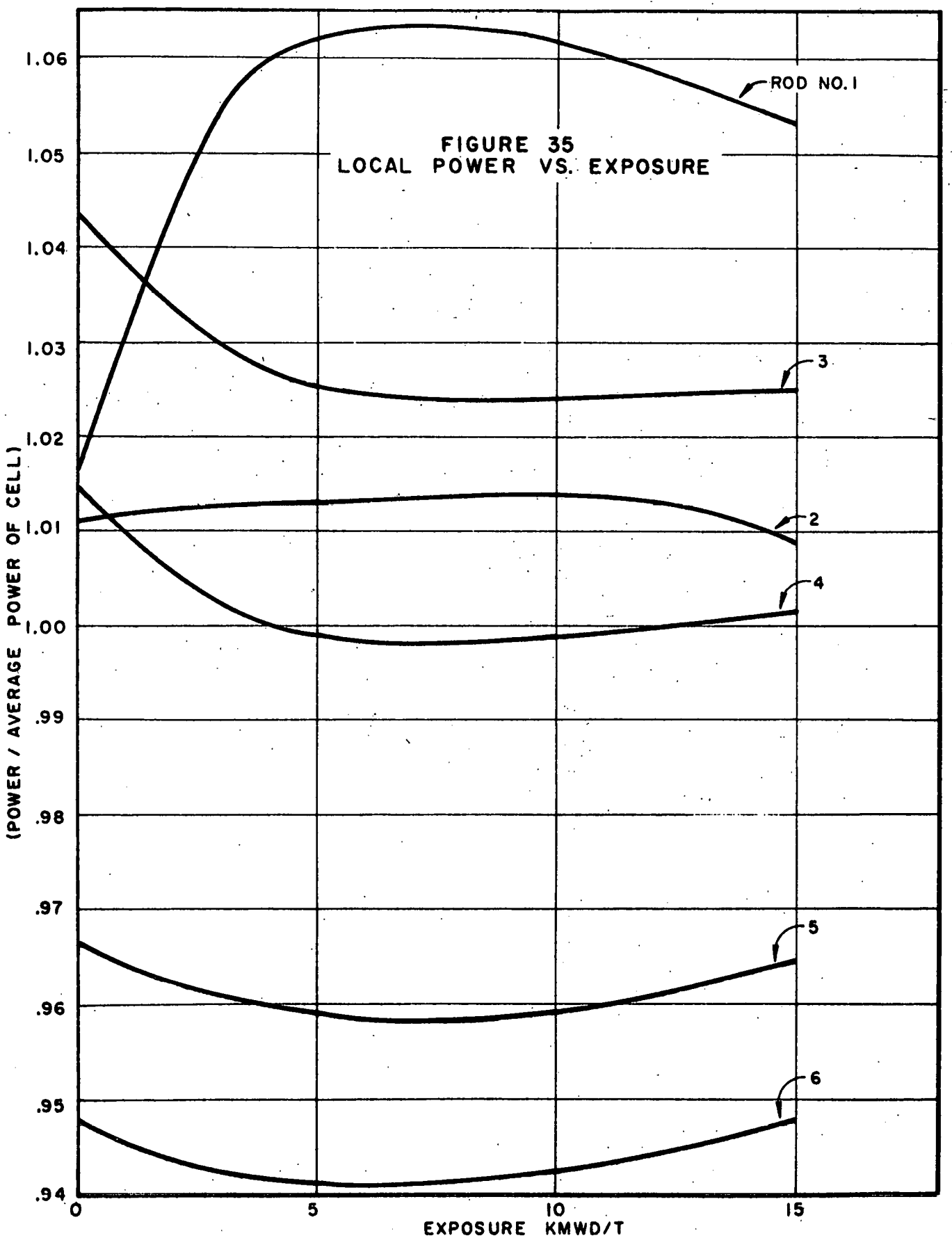

FIGURE 35
LOCAL POWER VS. EXPOSURE

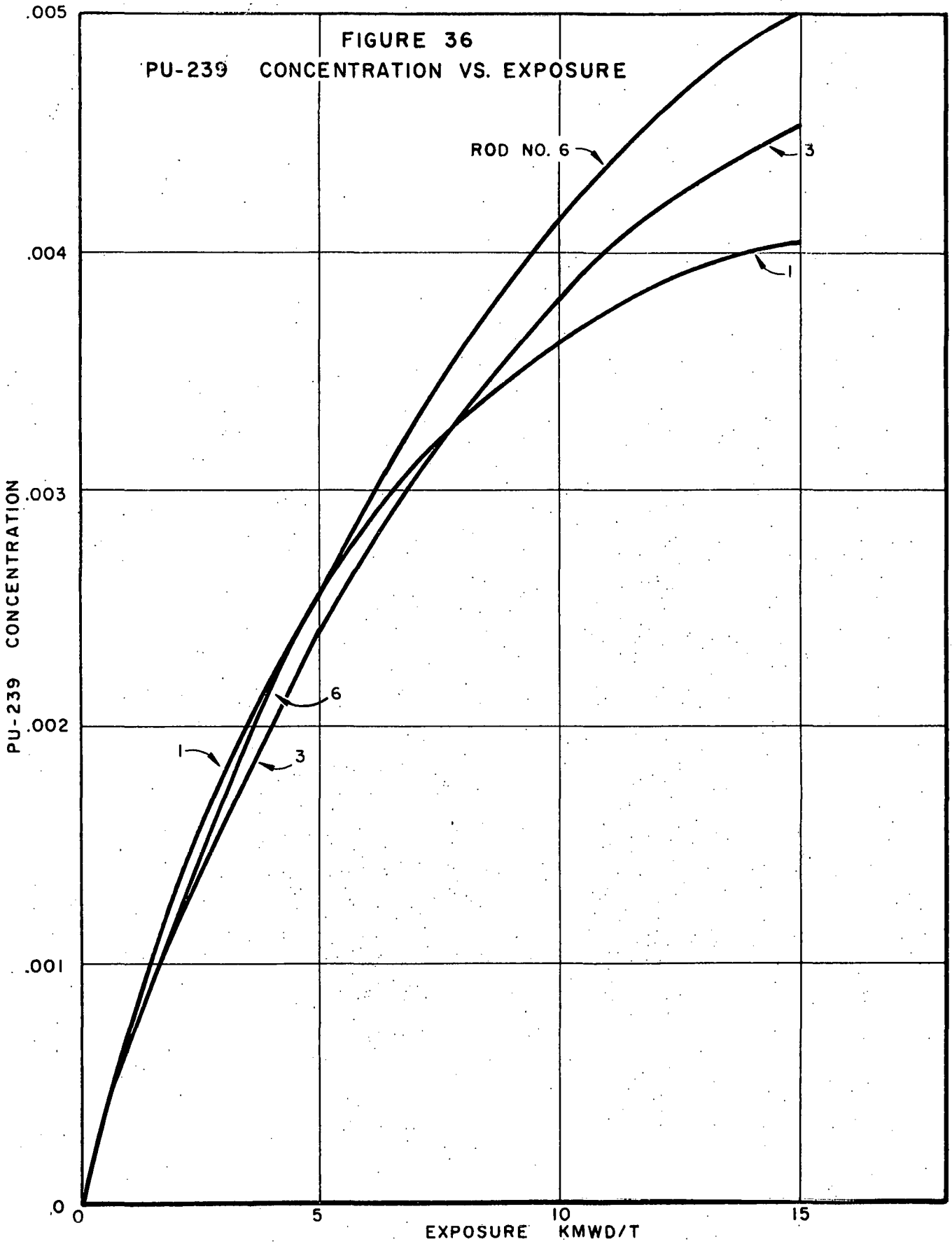
FIGURE 36
PU-239 CONCENTRATION VS. EXPOSURE
ROD NO. 6
3
1
6
1
3
.005
.004
.003
.002
.001
0
PU-239 CONCENTRATION
0
5
10
15
EXPOSURE KMWD/T

FIGURE 37
RELATIVE POWER WITH CONTROL ROD PATTERN CHANGES

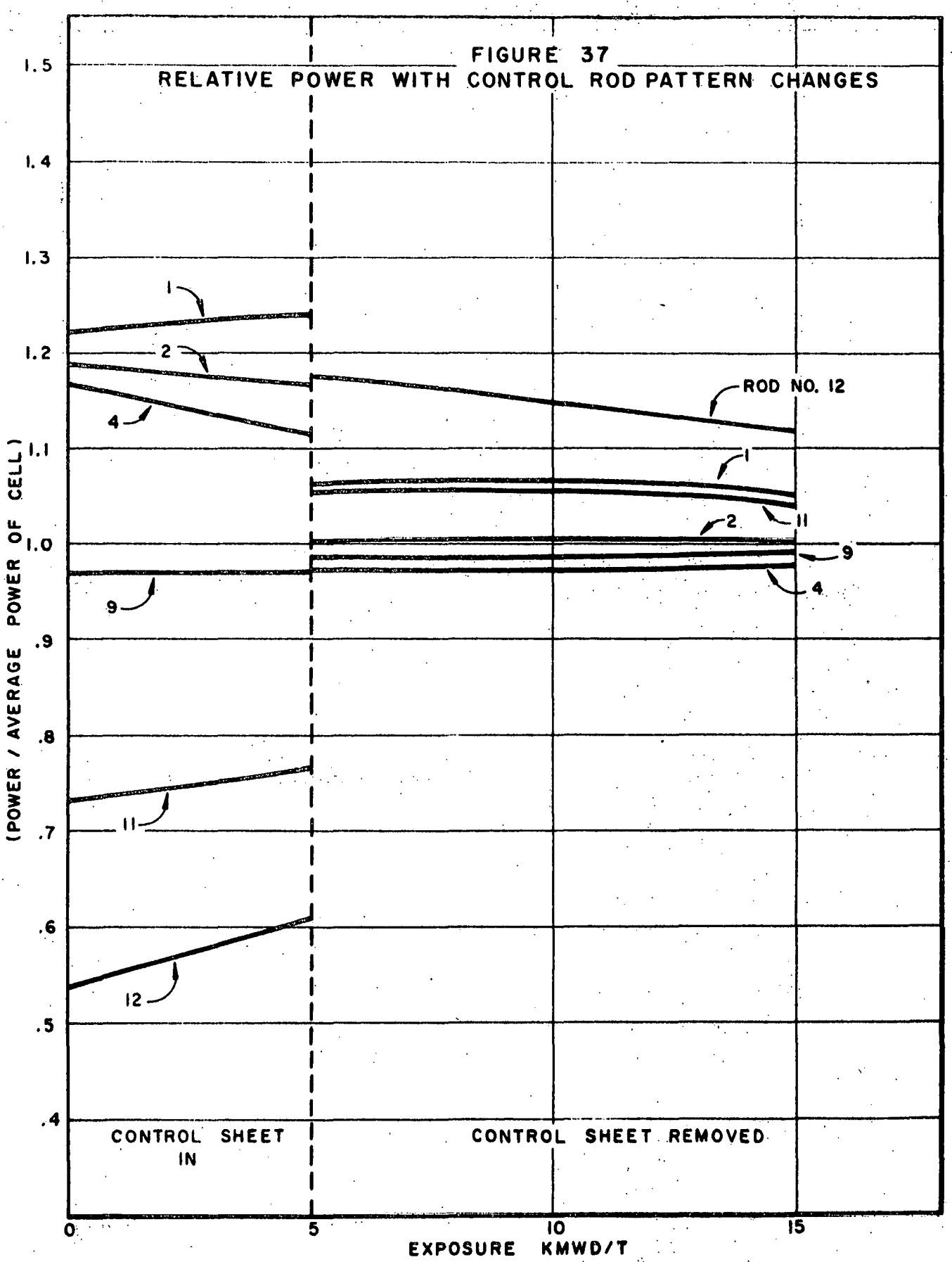

been to cause an increase in the local peaking factor from about 1.06 to 1.18. Two conclusions might be drawn from this calculation. First, there is an incentive for rotating control rod patterns during operation in order to minimize the shielding effects of the blades on adjacent fuel rods. Second, the perturbing influences of previous history may well dictate a lower limit on initial local power flattening below which it is not practical to go.

The method used in calculating this time dependence of the power distribution was to calculate the burnup of each fuel rod type with a point (zero dimensional) burner and combine the resultant cross sections in a one-dimensional diffusion theory calculation at specified time intervals. In this calculation, it is necessary to establish boundary conditions to be applied to the point burnup calculation. The basic methods used in establishing group constants for the three neutron energy group are described in the previous report(3).

3. EFFECT OF FUEL CYCLING ON GROSS RADIAL POWER DISTRIBUTIONS

One-dimensional calculations have been made of the gross radial power distribution in a typical 300 MW high power density reactor. The objective of this study is to find the effects of refueling schedules on radial power shapes. In all cases, a five-batch core refueling was assumed.

---

(3) Couchman, M. L., and Miller, C. L., "Analytical Methods for Consumers Research and Development Physics," GEAP 3574.

The power distributions and reactivities of several cases using an outside-in reshuffling pattern and different discharge exposures were examined. All cases studied assumed a five-batch refueling cycle. The results including the initial and final reactivities and peak to average power ratios are summarized in Table VII.

Table VII
Refueling Cycle Effects on Power Peaks and Reactivity

Discharge Exposure (MWD/T)	Refueling Cycle (MWD/T)	k_{eff} initial	k_{eff} final	Peak/Ave. initial	Peak/Ave. final
25,000	5,000	1.058	-----	1.437	-----
20,000	4,000	1.077	1.032	1.335	1.361
15,000	3,000	1.102	1.067	1.263	1.255
10,000	2,000	1.129	1.105	1.226	1.226

In these cases, it was assumed that the burnup increments were equal in each region. This would have been correct had there been a truly flat power distribution; however, this was not the case and therefore it was necessary to consider the effect of the power distribution on the exposure. This was done in a later phase of the study.

As the time duration of the refueling cycle is increased and therefore the discharge exposure increases, the radial peak to average power ratio tends to increase. This results from the low power generated near the core center caused by the low reactivity of the high exposure discharge fuel. This effect can be seen in Table VII.

A case, which combined a reasonable discharge exposure and a relatively low peak to average power ratio, was chosen for further study. Power distribution and reactivities were then calculated using a fixed discharge exposure of 15,000 MWD/T and a fixed reshuffling cycle of 3,000

MWD/T. In these cases, the reshuffling patterns were varied to determine the effects of the position of the different batches of fuel. Again five-batch refueling was assumed. The data for these cases is given in Table VIII. In this table, Region 1 is the innermost region, Region 2, the next region outward, etc. Figures 38 and 39 are curves showing the power distributions resulting from Cases 1 and 4 of Table VIII. It can be seen from Table VIII and Figures 38 and 39 that the distribution of fuel batches in the core has an important effect on the power distribution. For example, in comparing Case 4 and Case 5 in Table VIII where two adjacent batches were interchanged, the peak to average power ratio increased from 1.28 to 2.56. Therefore, it appears that considerable care should be exercised in following a particular reshuffling pattern as deviations from this pattern can cause serious effects.

TABLE VIII
Variable Refueling Cycle Effects on Power Peaks and Reactivity

	Exposure (1,000 MWD/T) in.						
Case	Region 1	Region 2	Region 3	Region 4	Region 5	k_{eff}	Peak/Ave.
1	6	12	3	9	0	1.112	2.328
2	9	6	12	3	0	1.103	1.460
3	9	12	6	3	0	1.100	1.157
4	12	6	9	3	0	1.102	1.278
5	6	12	9	3	0	1.108	2.558

One refueling pattern (Case 3 of Table VIII) was investigated in greater detail to find the power distribution in the equilibrium cycle. In obtaining the equilibrium power distribution, it was necessary to iterate between the burnup distribution and the power distribution until consistent results were obtained. The beginning and end of cycle effective reactivities and power ratios are shown in Table IX. Figure 40 shows the radial power

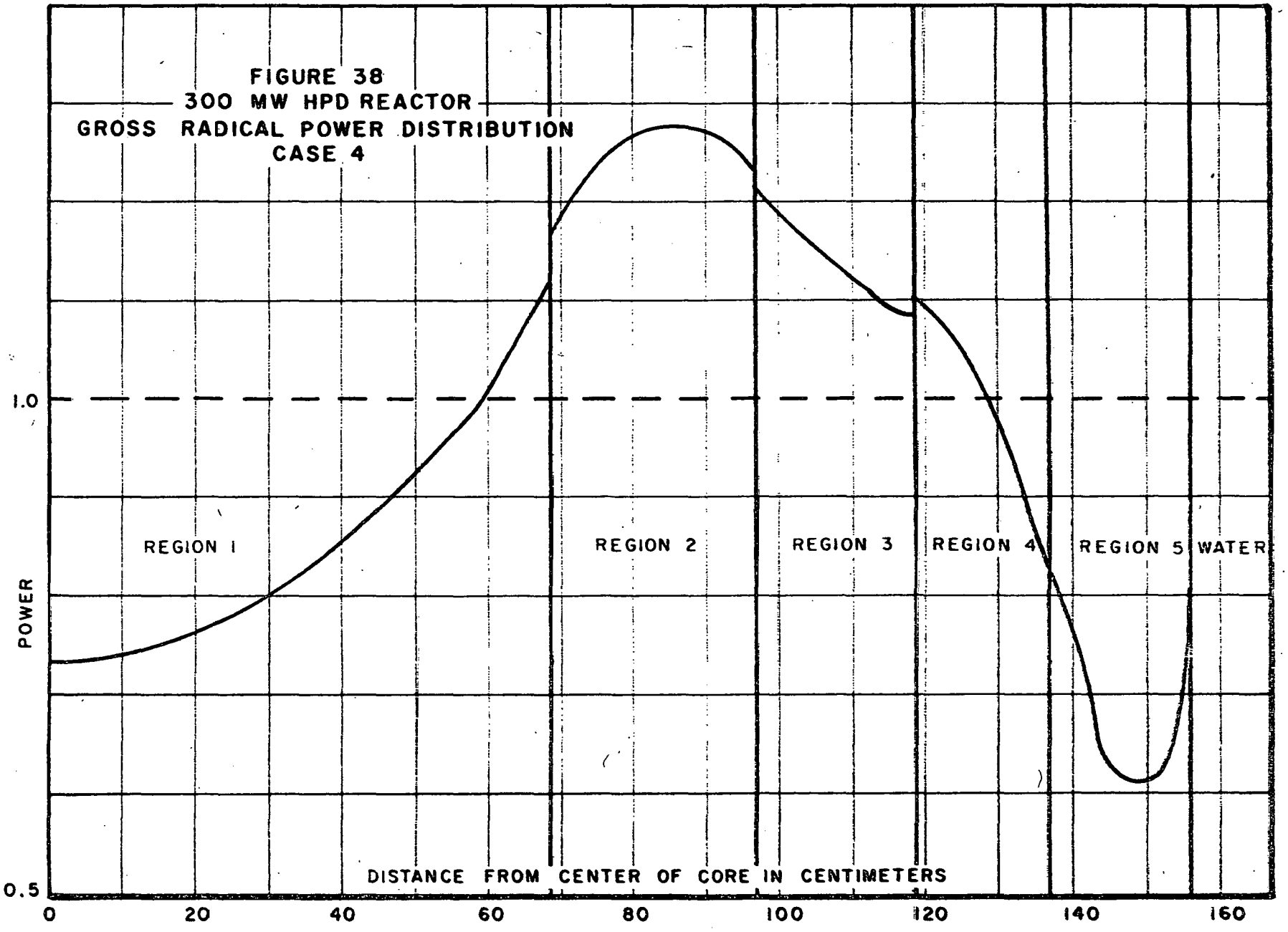
FIGURE 38
300 MW HPD REACTOR
GROSS RADICAL POWER DISTRIBUTION
CASE 4
1.0
0.5
POWER
REGION 1
REGION 2
REGION 3
REGION 4
REGION 5 WATER
DISTANCE FROM CENTER OF CORE IN CENTIMETERS
0
20
40
60
80
100
120
140
160

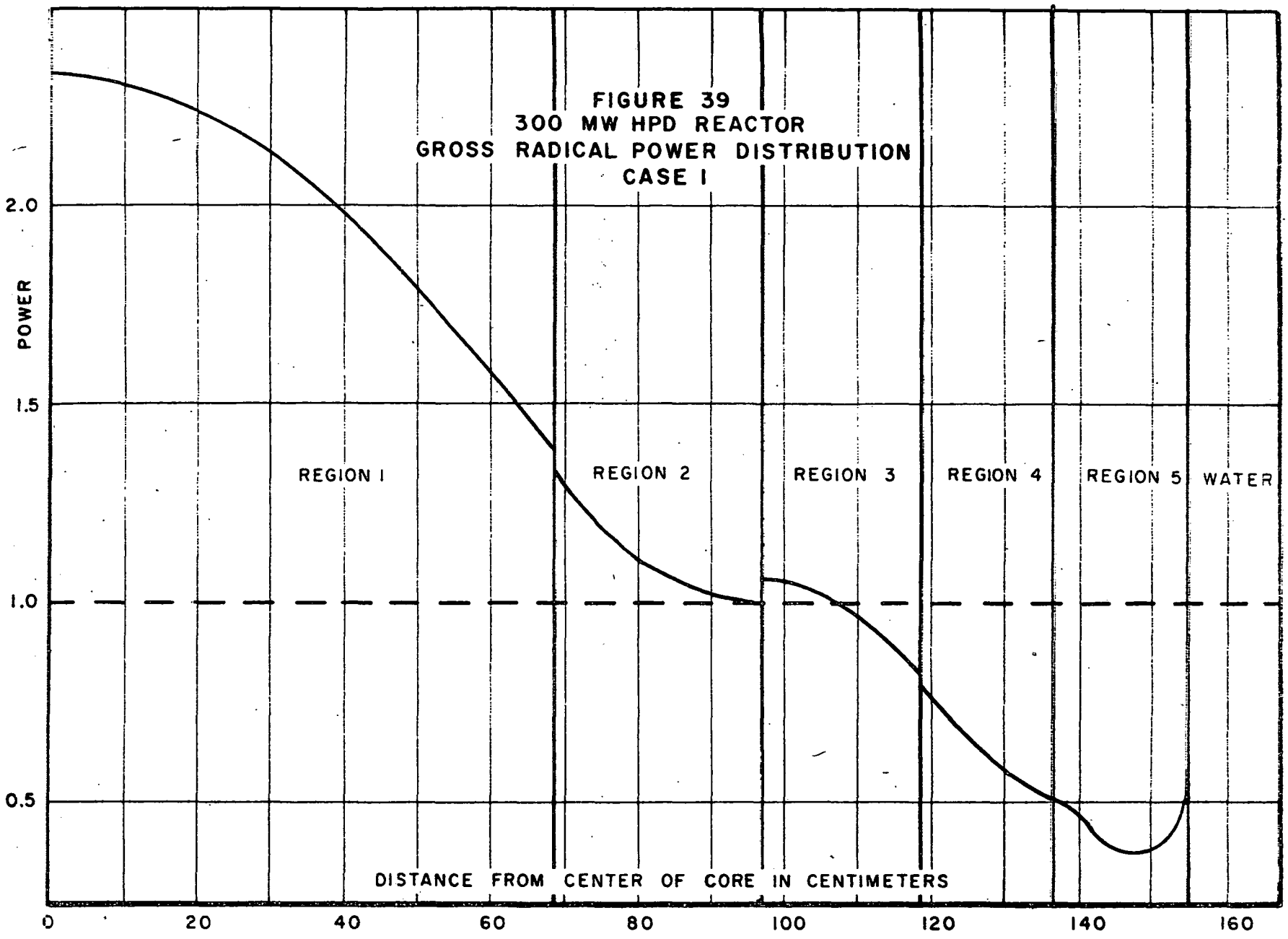
FIGURE 39
300 MW HPD REACTOR
GROSS RADICAL POWER DISTRIBUTION
CASE I
POWER
2.0
1.5
1.0
0.5
REGION 1
REGION 2
REGION 3
REGION 4
REGION 5
WATER
DISTANCE FROM CENTER OF CORE IN CENTIMETERS
0
20
40
60
80
100
120
140
160

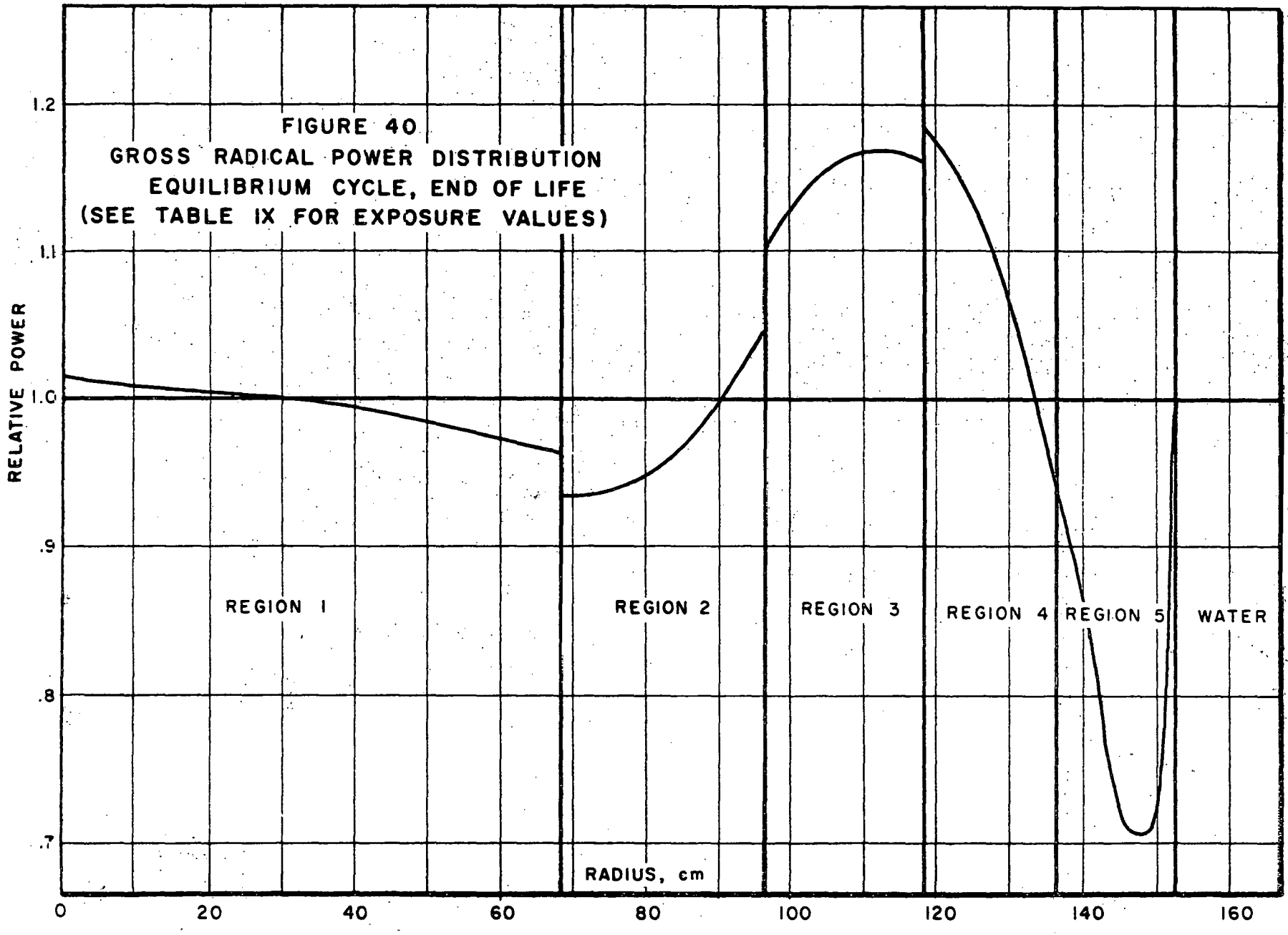
FIGURE 40
GROSS RADICAL POWER DISTRIBUTION
EQUILIBRIUM CYCLE, END OF LIFE
(SEE TABLE IX FOR EXPOSURE VALUES)
RELATIVE POWER
1.2
1.1
1.0
.9
.8
.7
REGION 1
REGION 2
REGION 3
REGION 4
REGION 5
WATER
RADIUS, cm
0
20
40
60
80
100
120
140
160

distribution at the end of an equilibrium cycle. This power distribution is not significantly different from that obtained previously under the assumption that the fuel had equal incremental burnup. It should be noted that the results obtained here are approximate in nature because they do not include the variation in axial effects or the variation in voids with radius. However, they do serve to show the importance of refueling schedules on operating power distributions and indicate that very desirable radial power shapes can be obtained by careful fuel schedules.

TABLE IX
Equilibrium Power Effective Reactivity and Power Ratios

Case	Exposure (MWD/T) in. Region 1	Region 2	Region 3	Region 4	Region 5	k_{eff}	Peak/Ave.
Beginning of Cycle	9,120	12,080	5,660	2,400	0	1.102	1.196
End of Cycle	12,080	15,000	9,120	5,660	2,400	1.065	1.183

4. LARGE HIGH POWER DENSITY CONCEPTUAL DESIGN

The development of physics technology for high power density cores is based on a conceptual design of a typical large (300 MWe) plant. Although tests may be performed in smaller reactors such as the Consumers Big Rock Power Plant, the values and incentives associated with potential design improvements will be referred to the larger core. As a starting point, the nuclear characteristics have been calculated for a large core design approximating recent technology. This design does not include features necessary to achieve power densities above those of the Big Rock Plant. It serves principally as a reference for use in evaluating the performance of future designs. These future designs are expected to demonstrate the overall goals of the development program.

The physics analysis of this initial conceptual design is being issued as a topical report [4]. Only a summary of the characteristics of this design will be given here.

The nuclear and thermodynamic characteristics of the core have not been investigated in as much detail as would be the case for a core being built. No attempt has been made to optimize the various design parameters at this stage. The constraints applied were that the core have a power density of 45 kw/l without exceeding a safe clad burnout margin or fuel center temperature limit, and be capable of satisfying the normal shutdown control requirements.

Whenever necessary in the course of design improvement studies, the characteristics of the reference core will be studied in greater detail. The physics data reported here is currently being employed to refine and expand the thermal-hydraulics treatment of the core.

A summary of the characteristics of the reactor is given below. (For more detail, see reference (4).

TABLE X
Summary of Reactor Characteristics

Plant Data	
Thermal Power	930 MW
Electrical Power	300 MW
Pressure	1,050 psia
Core Data	
Power Density	45 kw/l
Fuel	UO_2 (2.67 wt % U-235)

(4) Miller, C. L., "Large High Power Density Core - Interim Report I: Physics Description of Reference Design" - GEAP 3649.

Clad Material		Stainless Steel
Channel Material		Zircaloy-2
Number of Fuel Bundles		208
Number of Control Rods		97
Number of Fuel Rods		29,952
Active Core Height		108.5 inches
Core Volume		20.25×10^6 cm^3
Effective Core Diameter		120.4 inches
Water to UO_2 Volume Ratio		2.32
Specific Power		18.7 kw/kg U

Fuel Element Data

Fuel Rod O.D.	0.400 inch
Clad Thickness (304 Stainless Steel)	0.015 inch
Fuel Rods Per Bundle	144 in a 12 x 12 array
Zircaloy Channel Dimensions	6.51 inches I.D. 0.100 inches thick

Nuclear Data

k_∞ cold, Rods Out		1.235
k_∞ cold, Rods Inserted		0.952
k_∞ hot, Average Voids; Including Xe, Sm, Doppler Coefficient		1.183
Neutron Migration Area	Cold	37.34 cm^2
	Hot-Boiling	70.69 cm^2
Average Fuel Composition at 14,000 MWD/T		U-235 0.0134 atom fraction Pu-239 0.0036 atom fraction Pu-240 0.0011 atom fraction Pu-241 0.0005 atom fraction
Gross Power Peaking Factors	Axial	1.50
	Radial	1.30
Void Coefficient	20 °C	$-2.1 \times 10^{-3} \delta$k/k/% voids
Temperature Coefficient	20-50 °C	$-5.0 \times 10^{-5} \delta$k/k/°C

5. SCHEDULING COMPUTER

The principle incentives and the primary computer functions have been defined and in large measure detailed. A report[5] providing this detail and to serve as a basis for writing specifications for computer procurement has been completed and will be submitted for issuance pending AEC approval.

The computer's purpose is to make feasible higher power densities by operating closer to fuel element burnout limits, and to maximize fuel burnup. The incentives and functions of the scheduling computer will be summarized by item.

A. Incentive - The economic justification of a computer for fuel scheduling is largely based on freedom to peak neutron flux in the operating plant, the computer selecting the best schedule in terms of economics and operational limits. The studies made thus far indicate that the computer is not fully justified economically for a plant as small as the Big Rock Plant, based on fuel burnup maximization alone. However, a 300 MWe plant is estimated to permit a net saving of about 0.14 mills/kw. hr., or between $5,000 and $216,000 yearly, depending on average operating power and freedom to peak the flux. This freedom, of course, increases when the plant is operating at something less than rated power.

B. Reactor Heat Rate - The reactor heat rate is calculated from sensed data averaged over the specified period of thirty minutes and is logged for operator use as well as being made available for other computer calculations. Saturation enthalpies will be calculated from measured pressures; subcooled enthalpies will be determined from temperature and pressure measurements; and the pertinent flow rates will be measured directly or calculated from a combination of measured flows.

(5) E. S. Beckjord, "The Development of a Scheduling Computer for the Big Rock Plant," GEAP 3702.

The computer will be programmed to handle all normal operating conditions, e.g., a pressure range of 1000 to 1500 psia.

C. Ion Chamber Normalization and Calibration - Normalization is the process of relating thermal power to ion chamber readings and will be performed every half-hour following the heat rate calculation. The normalizing constant is determined by the ratio of heat rate to the product of average chamber reading and total fuel surface area. With this coefficient, evaluated half-hourly, the individual channel or volume heat flux can be determined. The equations describing these functions are:

$$\overline{R}_{core} = \frac{1}{36} \sum_{1}^{36} (WF)_i \; R_i$$

R_i is the individual chamber reading here weighted by a factor $(WF)_i$ determined from gamma probe data and stored in the computer. The normalizing constant is then,

$$K = \frac{\text{Heat Rate}}{\overline{R}_{Core} \times \text{Area}}$$

The individual channel heat flux can thereby be determined,

$$(q/A)_i = KR_i$$

Provision is made in the computer to by-pass faulty chamber signals or to accept operator input for the best local average factor.

Calibration is performed routinely with wire irradiation and much less frequently than the normalization. By comparing the individual chamber reading to normalized count ratio (R_i/C_i) to the average ratio $(\overline{R/C})$, each flux amplifier may be corrected to give a proper reading. The wire irradiation data (C_i) is read in manually as prepared from the counting equipment and corrected for the decay characteristic of the copper wire.

D. Reactor Core Performance - This series of calculations will provide the operator with current data regarding the principle operating limits. Heat flux, coolant temperatures, core pressure drop, and ion chamber readings are used to evaluate channel flow, nodal quality, nodal burnout ratio, nodal fuel center temperature, nodal heat flux, and pressure drop (inlet, exit, friction, acceleration, and elevation). These quantities are stored and printed on demand. Selected variables are printed as part of the regular log.

E. Neutron Flux Exposure - Effective maximization of burnup will depend in great part on accurate histories of the fuel, control rods, and ion chambers. The energy release per weight of channel section (3 sections), and the energy release weighted by the presence of voids will be kept, the latter to be used in plutonium buildup calculations. The ion chamber exposure histories will be individually kept, and control rod exposure will be determined daily based on the daily average power and average rod position and will be recorded for three sections of each rod on a cumulative basis. A log book identifying each fuel element, control rod, and ion chamber will be used to record cumulative exposures at times of removal, relocation, or as desired by the operator.

F. Burnup Maximization - This is the area of greatest incentive and the work is still in process to define adequately the best method of achievement. Studies have been made showing preferred power distributions for increased burnup. The strategy of operation is also found to be closely related to operating philosophy, whether it is operated as a base load plant or with a variable load schedule. The simplest scheme for implementing this on the computer requires the calculation on a general purpose computer (using exposure history as an input) of preferred flux distributions at specific operating conditions. These are then read into the scheduling

computer as local to average power ratios and control rod scheduling is evaluated in terms of actual to preferred ratios. These preferred distributions would be calculated externally perhaps each two to three months for incorporation in the plant computer.

Another scheme involving only the scheduling computer is now being studied. This will require development of concise and rapidly converging solutions of the coupled reactor flux, thermal, and hydraulic equations.

G. Control Rod Pattern Logic - The function of control rod pattern logic is to assist the reactor operator in control rod positioning from cold start-up through the operating range. The computer will print out on a typewriter near the operator the next rod position change for either increasing or decreasing power.

Sequences are evaluated periodically and stored in the computer. This may or may not be associated directly with the burnup maximization function. Typical sequences have been established for both the 50 and 75 MW Big Rock Core and have been determined without considering the maximization function. These are given in the detailed report.

H. Xenon Transient Calculations - As an aid to the operator near the end of core life, the reactivity requirements necessary to maintain power after a load change, with the subsequent xenon poisoning, will be calculated. This could be presented as either the rod motion to be expected in order to correct for the xenon poisoning, or as the incremental load change to be tolerated without loss of control due to xenon poisoning.

I. Plant Component Performance - Turbine heat rate, station heat rate, and condenser and feedwater heater performance characteristics can be easily incorporated in the monitoring function of the computer. Indication of

approaching equipment failure and comparative plant performance data will be made available from half-hourly computer calculations.

J. Instrumentation and Cabling - Most of the required input to the computer is derived from normal plant instrumentation. The interconnections required have been defined and the exceptions have been identified, with provision to add to the plant design or procure them with the computer. These are detailed in the Report, GEAP 3702, as is the accuracy and scanning rate associated with this input. The accuracy of computer calculations is related to the scanning rate, and the selected rate for principle calculations in the computer ~~is~~ sufficient to provide better than 90% confidence of calculational accuracy within the $\frac{1}{2}$% accuracy of the sensing instrumentation.

K. Input-Output - Based on the number of input signals involved and the computation required with the above accuracy, a calculation cycle of thirty minutes has been selected. Input is from analog and digital signals, from paper tape, computer console control, and from "on demand" control by the reactor operator. The output is by printed logs, information storage on punched tape, periodically typed information to the reactor operator, "on demand" information to the reactor operator, and console information monitoring computer operation. This function of input-output is still under investigation.

TASK IV - OPERATIONAL PLANNING AND TEST COORDINATION

1. TASK OBJECTIVE

This task is concerned with the test planning and design, safety assurance, test equipment procurement, operational scheduling for the R & D program, and maintaining and issuing reports on progress of the program.

2. SUMMARY OF WORK PERFORMED

The procurement of instrumentation and the preparation of test facilities at VBWR for the installation and operation of the two instrumented assemblies is 95% complete. These assemblies are currently scheduled to be inserted in the VBWR core about May 15, based on AEC approval of VBWR start-up by April 10.

Coordination of the R & D program with Design Engineering was maintained during this quarter. Safety valve requirements were established providing the necessary flexibility to operate safely at discreet reactor pressures ranging between about 800 psi and 1500 psi. Spare sets of valves and springs are being provided to meet this requirement. Instrumentation lead wire and signal cable requirements have been established for rod oscillation testing, computer input-output and instrumented assembly tests.

Reports that have been issued during this quarter include two Monthly Progress Letters, numbers 12 and 13, for January and February; the Third Quarterly Progress Report, GEAP 3632; and the topical report "The Design and Fabrication of High Power Density Fuel Assemblies for VBWR Irradiation Testing," GEAP 3609, by J. W. Lingafelter and W. D. Fowler. Two topical reports have been prepared for issuance subject to AEC approval as follows:

"Swaging Over Unground Pellets" GEAP 3623
by R. L. Brown

"Large High Power Density Core - Interim Report I: GEAP 3649
Physics Description of Reference Design"

by C. L. Miller

3. VBWR SCHEDULE

The irradiation of the fuel elements fabricated under Task IA and IB will be resumed in VBWR with the approval by the AEC of VBWR operation. An April 10 date of approval is presumed though not firm. Based on receipt of approval the following schedule is that expected to be followed in bringing the VBWR to power operation.

Days After AEC Approval	
0 - 9	Load core, make pre-operational checks and measurements.
10 - 19	Start-Up; make hot critical tests and complete 30 MW Nuclear Start-up tests.
20 - 27	Full power, steady-state operation.
28 - 31	Shutdown: Charge one Dresden and five Consumers elements. Install flux wires, repair steam leaks.
32	Flux wire irradiation.
33 - 40	Shut down; install prototype B_4C Control rod and two instrumented assemblies, remove flux wires, move new assemblies to final desired power locations in core.
41 - 62	Operate steady-state, full power.
63 - 66	Add SADE defect element SADE I, one Consumers HPD special element and two Fuel Cycle special development assemblies.
67 - 90	Operate SADE defect test.